Eocene–Early Miocene paleotopography of the Sierra Nevada–Great Basin–Nevadaplano based on widespread ash-flow tuffs and paleovalleys

Christopher D. Henry[1], Nicholas H. Hinz[1], James E. Faulds[1], Joseph P. Colgan[2], David A. John[2], Elwood R. Brooks[3], Elizabeth J. Cassel[4], Larry J. Garside[1], David A. Davis[1], and Steven B. Castor[1]
[1]*Nevada Bureau of Mines and Geology, University of Nevada, Reno, Nevada 89557, USA*
[2]*U.S. Geological Survey, Menlo Park, California 94025, USA*
[3]*California State University, Hayward, California 94542, USA*
[4]*Department of Earth and Environment, Franklin & Marshall College, Lancaster, Pennsylvania 17604, USA*

ABSTRACT

The distribution of Cenozoic ash-flow tuffs in the Great Basin and the Sierra Nevada of eastern California (United States) demonstrates that the region, commonly referred to as the Nevadaplano, was an erosional highland that was drained by major west- and east-trending rivers, with a north-south paleodivide through eastern Nevada. The 28.9 Ma tuff of Campbell Creek is a voluminous (possibly as much as 3000 km^3), petrographically and compositionally distinctive ash-flow tuff that erupted from a caldera in north-central Nevada and spread widely through paleovalleys across northern Nevada and the Sierra Nevada. The tuff can be correlated over a modern area of at least 55,000 km^2, from the western foothills of the Sierra Nevada to the Ruby Mountains in northeastern Nevada, present-day distances of ~280 km west and 300 km northeast of its source caldera. Corrected for later extension, the tuff flowed ~200 km to the west, downvalley and across what is now the Basin and Range–Sierra Nevada structural and topographic boundary, and ~215 km to the northeast, partly upvalley, across the inferred paleodivide, and downvalley to the east. The tuff also flowed as much as 100 km to the north and 60 km to the south, crossing several east-west divides between major paleovalleys. The tuff of Campbell Creek flowed through, and was deposited in, at least five major paleovalleys in western Nevada and the eastern Sierra Nevada. These characteristics are unusual compared to most other ash-flow tuffs in Nevada that also flowed great distances downvalley, but far less east and north-south; most tuffs were restricted to one or two major paleovalleys. Important factors in this greater distribution may be the great volume of erupted tuff and its eruption after ~3 Ma of nearly continuous, major pyroclastic eruptions near its caldera that probably filled in nearby topography.

Distribution of the tuff of Campbell Creek and other ash-flow tuffs and continuity of paleovalleys demonstrates that (1) the Basin and Range–Sierra Nevada structural and topographic boundary did not exist before 23 Ma; (2) the Sierra Nevada was a lower, western ramp to the Nevadaplano; and (3) any faulting before 23 Ma in western Nevada, including in what is now the Walker Lane, and before 29 Ma in northern Nevada as far east as what is now the Ruby Mountains metamorphic core complex, was insufficient to disrupt the paleodrainages. These data are further evidence that major extension in Nevada occurred predominantly in the late Cenozoic.

Characteristics of paleovalleys and tuff distributions suggest that the valleys resulted from prolonged erosion, probably aided by the warm, wet Eocene climate, but do not resolve the question of the absolute elevation of the Nevadaplano. Paleovalleys existed at least by ca. 50 Ma in the Sierra Nevada and by 46 Ma in northeastern Nevada, based on the age of the oldest paleovalley-filling sedimentary or tuff deposits. Paleovalleys were much wider (5–10 km) than they were deep (to 1.2 km; greatest in western Nevada and decreasing toward the paleo–Pacific Ocean) and typically had broad, flat bottoms and low-relief interfluves. Interfluves in Nevada had elevations of at least 1.2 km because paleovalleys were that deep. The gradient from the caldera eastward to the inferred paleodivide had to be sufficiently low so that the tuff could flow upstream more than 100 km. Two Quaternary ash-flow tuffs where topography is nearly unchanged since eruption flowed similar distances as the mid-Cenozoic tuffs at average gradients of ~2.5–8 m/km. Extrapolated 200–300 km (pre-extension) from the Pacific Ocean to the central Nevada caldera belt, the lower gradient would require elevations of only 0.5 km for valley floors and 1.5 km for interfluves. The great eastward, upvalley flow is consistent with recent stable isotope data that indicate low Oligocene topographic gradients in the Nevadaplano east of the Sierra Nevada, but the minimum elevations required for central Nevada are significantly less than indicated by the same stable isotope data.

Although best recognized in the northern and central Sierra Nevada, early to middle Cenozoic paleodrainages may have crossed the southern Sierra Nevada. Similar early to middle Cenozoic paleodrainages existed from central Idaho to northern Sonora, Mexico, and persisted over most of that region until disrupted by major Middle Miocene extension. Therefore, the Nevadaplano was the middle part of an erosional highland that extended along at least this length. The timing of origin and location of this more all-encompassing highland indicates that uplift was predominantly a result of Late Cretaceous (Sevier) contraction in the north and a combination of Late Cretaceous–early Cenozoic (Sevier and Laramide) contraction in the south.

INTRODUCTION

It is now well established that the Great Basin (western United States) was an erosional highland in the middle Cenozoic, following crustal thickening during Mesozoic–early Cenozoic shortening, batholith emplacement, and shallow slab subduction (e.g., Dilek and Moores, 1999; Humphreys et al., 2003; DeCelles, 2004;

Geosphere; February 2012; v. 8; no. 1; p. 1–27; doi:10.1130/GES00727.1; 11 figures; 2 tables.

Dickinson, 2006; Best et al., 2009; Cassel et al., 2009a, 2009b; Colgan and Henry, 2009; Ernst, 2010; Henry and Faulds, 2010). Major river systems drained this highland both west to the Pacific Ocean and east to the Uinta Basin (Fig. 1; Henry, 2008; Cassel et al., 2009a, 2009b; Henry and Faulds, 2010). The absolute elevation and structural-topographic evolution of this highland in the mid-Cenozoic remain highly controversial, however, particularly the paleoelevation of what is now the Sierra Nevada (Wakabayashi and Sawyer, 2001; Mulch et al., 2006, 2008; Cassel et al., 2009a, 2009b; Molnar, 2010) and the timing of extension in northeastern Nevada, especially around the Ruby Mountains–East Humboldt Range metamorphic core complex (McGrew and Snee, 1994; Snoke et al., 1997; McGrew et al., 2000; Howard, 2003; Colgan and Henry, 2009; Druschke et al., 2009; Colgan et al., 2010; Henry et al., 2011; Mix et al., 2011).

An ancestral Sierra Nevada probably formed during arc magmatism (Wernicke et al., 1996), and these batholithic rocks were exhumed during the Late Cretaceous–early Cenozoic (Dumitru, 1990; House et al., 1997; Cecil et al., 2006). Based on stable isotope and organic molecule paleothermometry and altimetry, together with detrital zircon geochronology, the Eocene–Oligocene Sierra Nevada is interpreted to have been at approximately the same elevation (~2.5–3 km at the latitude of Lake Tahoe) as it is today (Horton et al., 2004; Mulch et al., 2006, 2008; Cassel et al., 2009a, 2009b; Cecil et al., 2010; Hren et al., 2010). In contrast, Huber (1981), Unruh (1991), Wakabayashi and Sawyer (2001), Jones et al. (2004), Stock et al. (2004, 2005), and Clark et al. (2005) concluded from dated stream incision and gradients that the Sierra Nevada was much lower in the Eocene (≤1 km) and attained its present elevation following 1.5–2.5 km of uplift during the Late Miocene and Pliocene. Numerical models of bedrock channel erosion support two episodes of uplift, in the Late Cretaceous or middle Cenozoic, and the Late Miocene (Pelletier, 2007). Provenance studies and the distribution of ash-flow tuffs and paleovalleys unequivocally demonstrate that Eocene–Oligocene rivers drained from central Nevada across the northern and central Sierra Nevada to the Pacific Ocean, but these data do not constrain the absolute surface elevation of the Sierra Nevada at the time (Bateman and Wahrhaftig, 1966; Yeend, 1974; Faulds et al., 2005; Garside et al., 2005; Henry, 2008; Henry and Faulds, 2010; Cassel et al., 2012b). In contrast, Cecil et al. (2010) and Lechler and Niemi (2011) interpreted the predominance of Mesozoic, i.e., Sierra Nevada batholith age, detrital zircons in Eocene sedimentary deposits of the Sierra Nevada to indicate that the Eocene headwaters were in the modern Sierra Nevada, not in central Nevada.

Further complicating matters, the northern and southern Sierra Nevada may have undergone different uplift histories. For example, foundering of a dense, eclogitic root to the Sierra Nevada batholith has been called upon to generate Pliocene uplift and distinctive mafic alkalic magmatism of the southern Sierra Nevada (Ducea and Saleeby, 1998; Farmer et al., 2002; Saleeby et al., 2003; Jones et al., 2004; Zandt et al., 2004; Figueroa and Knott, 2010). The lack of similar distinctive magmatism in the northern Sierra Nevada suggests that delamination-triggered uplift is unlikely to have occurred there (Cousens et al., 2008, 2011).

In this paper we use the Oligocene tuff of Campbell Creek as a particularly good example of a widespread ash-flow tuff in the Great Basin and Sierra Nevada, the distribution of which bears on the topography, relief, and evolution of the Nevadaplano. We combine these data with published information to place constraints on the origin of the Nevadaplano and the overall extent of the related highlands to the north and south.

TUFF OF CAMPBELL CREEK

Correlation: Petrography, Chemical Composition, Age, and Remanent Magnetization

The 28.9 Ma tuff of Campbell Creek is a petrographically and compositionally distinctive ash-flow tuff that erupted from a caldera in north-central Nevada and spread widely in paleovalleys across northern Nevada and the eastern Sierra Nevada (Fig. 1). Correlation of the tuff, also called the C unit of the Bates Mountain Tuff in central Nevada (Gromme et al., 1972), from the Sierra Nevada to northeastern Nevada is based on its stratigraphic position, distinctive phenocryst assemblage, composition, $^{40}Ar/^{39}Ar$ age, and paleomagnetic direction (Figs. 2 and 3; Tables 1 and 2). The tuff contains ~5%–10% phenocrysts of sanidine, plagioclase, distinctively vermicular (resorbed) quartz, and biotite (Fig. 4). Large glass shards as much as 1 mm diameter and glass lumps to ~1 cm diameter are common.

All but the most distal sections, regardless of their thickness, show welding and crystallization zoning typical of ash-flow tuffs (Fig. 5). A 1–3-m-thick, poorly welded glassy base passes upward to a densely welded vitrophyre, which is black to white depending on the degree of hydration (Fig. 5B). Most of the tuff is densely welded and devitrified. An upper nonwelded zone was probably common before erosion, but is preserved in only a few locations. Only the most distal sections, Skillman Flat, Welches Canyon, and East Humboldt Range (Figs. 1 and 5C), are poorly welded and glassy throughout. Large pumice fragments, as much as 30 cm long, are common (Figs. 5D–5F). As with many other tuffs in western Nevada (Henry and Faulds, 2010), the tuff of Campbell Creek commonly shows primary dips where it compacted against moderate to steep topography in paleovalleys (Fig. 5D). The tuff of Campbell Creek is slightly to rarely moderately rheomorphic within the caldera and in several proximal locations. Stretched pumice is the most common rheomorphic feature.

The tuff of Campbell Creek is a compositionally nearly homogeneous, high-SiO_2 rhyolite with 75–77% SiO_2. Major elements vary little, whereas trace elements show greater variation (Figs. 2 and 3). Whole-rock samples from this study and from those of Brooks et al. (2003, 2008) have nearly identical compositions; minor differences probably reflect differences in analytical methods. Analytical bias is apparent in P_2O_5 and Nb, which are systematically higher in the Brooks et al. (2003, 2008) data set from Haskell Peak. Two whole-rock samples from Haskell Peak analyzed for this study have P_2O_5 and Nb concentrations similar to all other tuff of Campbell Creek samples.

Both major and trace elements of basal and upper samples of outflow tuff from individual sections are indistinguishable. Two individual pumice samples (H09-63, H09-65) from the Reese River Narrows section are indistinguishable from each other and from two bulk samples (H01-139, H01-140). Variations in the more mobile oxides (Na_2O, K_2O, CaO, MgO) most likely reflect hydration of nonwelded vitrophyres, especially in the westernmost (H07-230, Skillman) and easternmost (H07-95, H10-79; Welches Canyon, East Humboldt Range) distal, nonwelded, and strongly hydrated vitrophyres.

Despite the lack of observed compositional variation in individual sections, trace elements for the entire group of samples vary, and a few dacite pumice fragments are present in intracaldera tuff. Total Zr concentration ranges from 136 to 83 ppm (mostly ≥98 ppm) in whole-rock samples and is as low as 76 ppm in glass shards (analyzed by Cassel et al., 2009a). This range probably results from crystallization and separation of zircon and allows use of Zr as an indicator of magma evolution. Samples with high Zr concentrations (H07-230 and H01-61) are least evolved, whereas samples with the lowest Zr concentrations (H08-35 and the shard samples of Cassel et al., 2009a) are most evolved. TiO_2, Sr, Ba, Eu, and Hf decrease linearly with decreasing Zr, whereas Rb and Th increase.

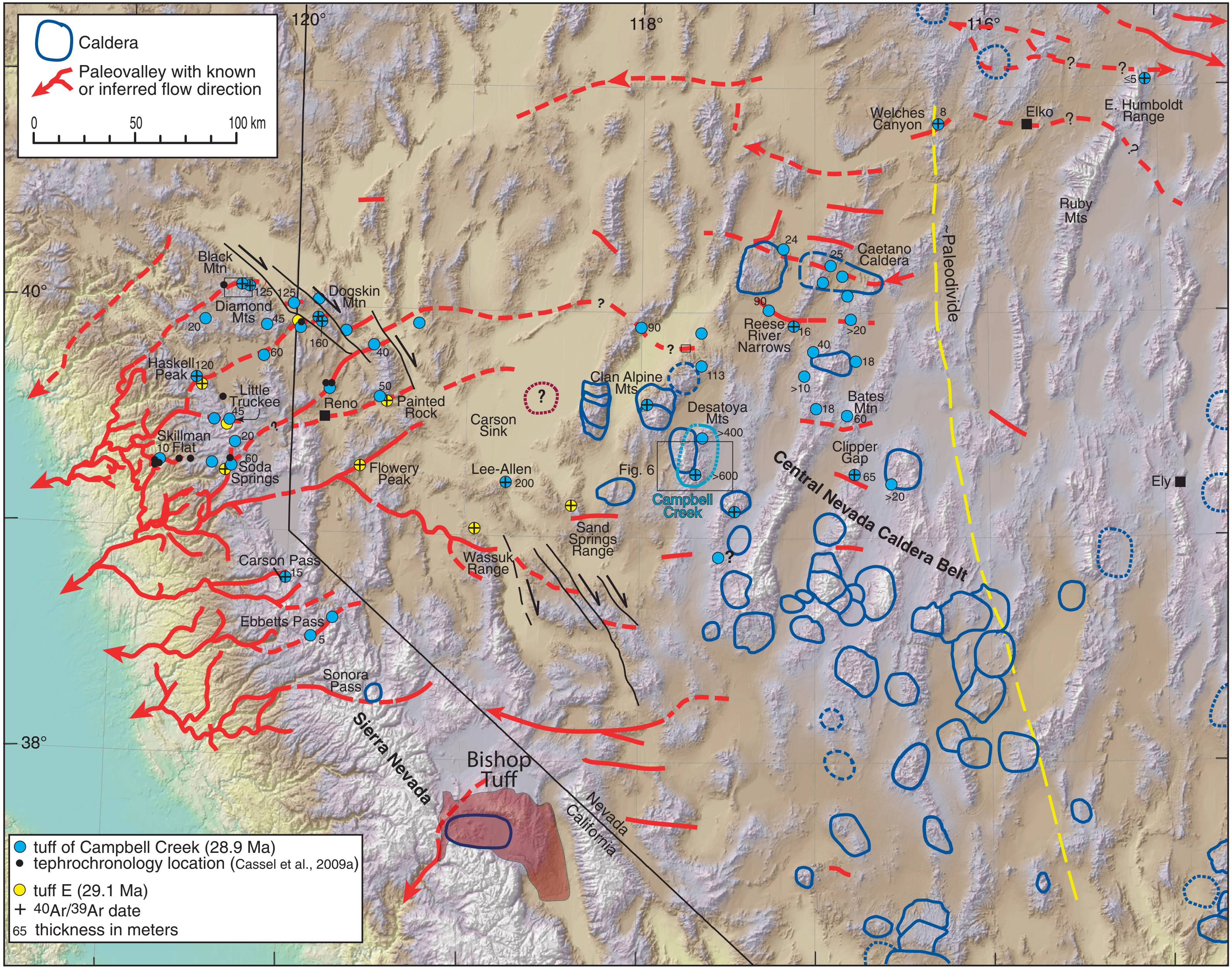

Figure 1. Digital elevation map of western Nevada and the Sierra Nevada showing the distribution of known paleovalleys, including segments (from Lindgren, 1911; Jenkins, 1932; Faulds et al., 2005; Garside et al., 2005; Henry and Faulds, 2010), a proposed paleodivide (Henry, 2008), and known locations of the tuff of Campbell Creek and probably related underlying tuff E. The tuff of Campbell Creek erupted from the Campbell Creek caldera in the Desatoya Mountains and flowed as much as 200 km westward down paleovalleys. In contrast, the 760 ka Bishop Tuff erupted at the western margin of the Basin and Range and flowed a maximum of ~50 km into basins to the north, northeast, and southeast (Bailey, 1989). The queried caldera in the Carson Sink is the suggested possible source of the Nine Hill Tuff (Best et al., 1989).

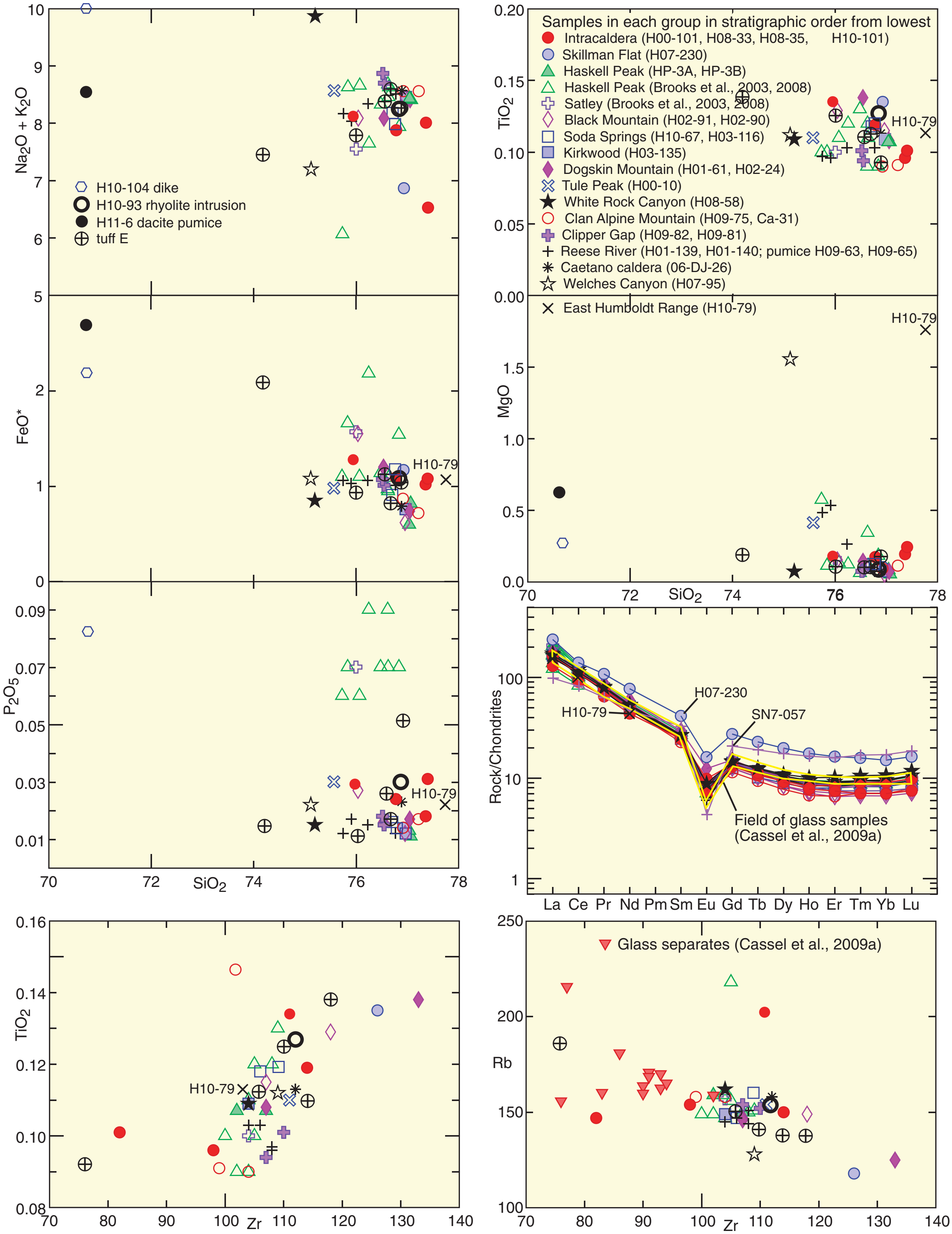

Figure 2. Plots of major elements, rare earth elements (REEs; normalization values from Sun and McDonough, 1989), and Zr illustrating narrow compositional range of high-SiO_2 rhyolitic tuff of Campbell Creek. Major elements show essentially no zoning, whereas trace elements, especially Zr, show some zoning. TiO_2, Sr, Ba, Eu, and Hf decrease linearly with decreasing Zr, whereas Rb and Th increase (only TiO_2 and Rb shown). H10-79 is sample from easternmost occurrence in East Humboldt Range (Fig. 1).

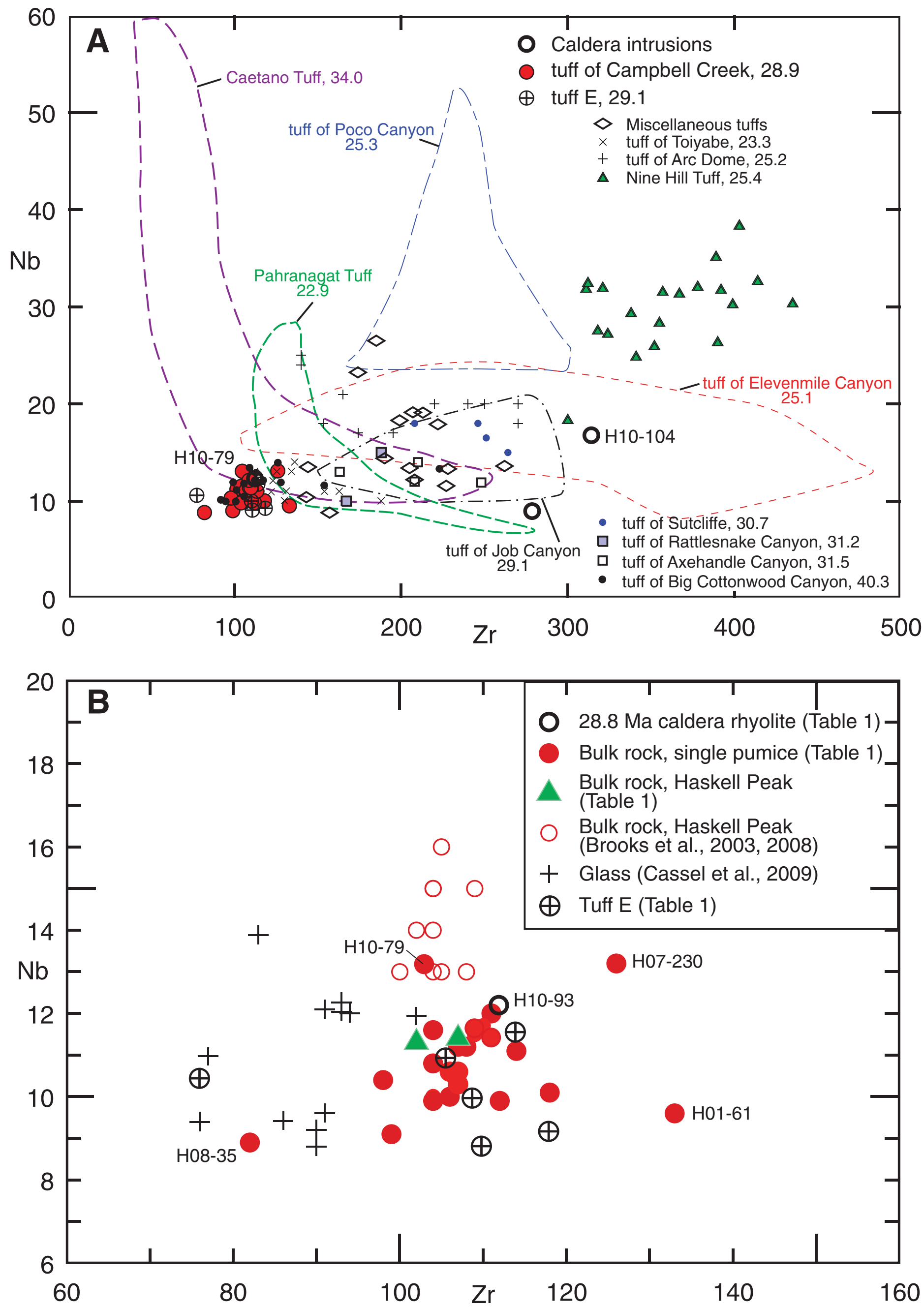

Figure 3. Plots of Zr versus Nb. (A) Tuff of Campbell Creek and related tuff E have distinctive low Zr and Nb concentrations compared to other ash-flow tuffs of the ignimbrite flareup of Nevada. Comparison data are from Deino (1985), John (1992, 1995), Best et al. (1995), and Henry (2008). (B) Tuff of Campbell Creek data. Higher Nb concentrations in analyses from Brooks et al. (2003, 2008) suggest a systematic bias. Lower Zr concentrations in glass separates (Cassel et al., 2009a) probably reflect presence of zircon in the whole-rock samples.

These patterns probably indicate fractionation of titanomagnetite or ilmenite and plagioclase ± sanidine, all of which are present in the tuff of Campbell Creek.

Sparse, large dacite or low-SiO_2 rhyolite pumice fragments present in intracaldera tuff also indicate compositional variation (Fig. 5F; Table 1). These pumice fragments are more abundantly porphyritic than the host rhyolite, with as much as 40% phenocrysts, mostly of plagioclase, with lesser sanidine, biotite, minor vermicular quartz, and sparse hornblende. The dacite has significantly greater TiO_2, Al_2O_3, FeO, MgO, CaO, Sr, Zr, and Ba and lower SiO_2, Rb, Nb, Th, and U abundances than the main rhyolite (Table 1; H11-6).

We interpret the compositional variation of the entire group of samples, but the lack of variation in individual sections to indicate that different ash flows tapped different parts of a compositionally heterogeneous magma chamber. These different ash flows either did not all flow to the same locations, or mixed sufficiently to homogenize before deposition, or a combination of both. For example, the 4-km-thick intracaldera Caetano Tuff, whose caldera is 110 km northeast of the Campbell Creek caldera (Fig. 1), is zoned from high- to low-SiO_2 rhyolite and is even more strongly zoned in trace elements, whereas outflow sections show little zoning (John et al., 2008a, 2008b). More comprehensive study of the intracaldera tuff of Campbell Creek, which might preserve more complete zonation, would be worthwhile.

The tuff of Campbell Creek is distinct relative to other tuffs in the Great Basin in having low concentrations of Zr (~80–130 ppm) and Nb (~9–13 ppm) (Fig. 3; John, 1992; Deino, 1985; Best et al., 1995; Maughan et al., 2002; Brooks et al., 2003, 2008; Henry, 2008). Higher Zr concentrations in whole-rock samples compared to glass shards probably reflect presence of zircon in the whole-rock samples. This interpretation is supported by the linear relationship between Zr and Hf, which is incorporated in zircon by simple substitution for Zr (Hoskin and Schaltegger, 2003). Two Great Basin ash-flow tuffs with Zr and Nb concentrations similar to those of the tuff of Campbell Creek can be distinguished in other ways. The tuff of Toiyabe, the distribution of which partly overlaps that of the tuff of Campbell Creek, is abundantly porphyritic and 23.3 Ma (John, 1992; Henry and Faulds, 2010). The tuff of Big Cottonwood Canyon is petrographically similar to the tuff of Campbell Creek, but is 40.3 Ma and restricted to northeastern Nevada (Henry, 2008).

Over much of its distribution, the tuff of Campbell Creek is underlain by a slightly older but otherwise nearly indistinguishable tuff (Figs. 1, 2, and 3), informally referred to as tuff E (Brooks et al., 2003, 2008). Tuff E contains 10%–22% of the same phenocrysts as the tuff of Campbell Creek and is a high-SiO_2 rhyolite with similar major and trace element concentrations, including low Zr and Nb (Brooks et al., 2003, 2008). Tuff E can be distinguished from the tuff of Campbell Creek primarily by its stratigraphic position and slightly older $^{40}Ar/^{39}Ar$ age (29.2 Ma; Table 2), and to a lesser extent by its greater range in phenocryst abundance and less vermicular quartz phenocrysts that better

TABLE 1. CHEMICAL ANALYSES OF THE TUFF OF CAMPBELL CREEK AND RELATED ROCKS

	Tuff of Campbell Creek												
Sample	HP-3A	HP-3B	4_5B	2_3	18_3	2_4	FB	2_1	4_5F	20_3	2_2	14_1	H07-230
Location	Haskell Peak	Haskell Peak	Haskell Peak	Haskell Peak	Haskell Peak	Haskell Peak	Haskell Peak	Haskell Peak	Haskell Peak	Haskell Peak	Haskell Peak	Hwy 49, Sattley	Skillman Flat
Position	lower	upper	base	middle	top	top	base	base	base	middle	middle		
	vitrophyre	devitrified	devitrified	devitrified	devitrified	devitrified	vitrophyre	devitrified	vitrophyre	vitrophyre	devitrified	vitrophyre	vitrophyre
Latitude	39.67459	39.67459											39.31687
Longitude (W)	120.56212	120.56212											120.79657
SiO_2	77.07	77.04	75.73	75.84	76.84	76.25	76.64	76.63	76.62	76.07	76.48	76.00	76.93
TiO_2	0.107	0.107	0.1	0.1	0.09	0.12	0.11	0.12	0.09	0.11	0.13	0.1	0.135
Al_2O_3	12.89	13.09	15.29	12.60	12.43	12.59	12.56	12.57	12.66	13.04	12.98	13.48	14.35
FeO*	0.82	0.60	1.10	1.66	1.54	2.18	1.09	0.95	0.97	1.10	1.14	1.57	1.17
MnO	0.052	0.016	0.05	0.01	0.01	0.02	0.02	0.04	0.02	0.02	0.02	0.03	0.024
MgO	0.05	0.08	0.57	0.11	0.18	0.12	0.11	0.34	0.10	0.13	0.06	0.16	0.10
CaO	0.60	0.61	0.91	0.80	0.73	0.74	0.72	0.71	0.66	0.69	0.66	0.86	0.42
Na_2O	3.26	3.57	1.49	3.97	3.48	3.03	3.78	3.65	3.37	3.82	3.47	2.64	2.17
K_2O	5.15	4.86	4.58	4.66	4.46	4.62	4.85	4.81	5.31	4.84	4.86	4.91	4.70
P_2O_5	0.011	0.013	0.06	0.07	0.07	0.09	nd	0.07	0.09	0.06	0.07	0.07	0.014
LOI													
Total	94.43	96.86											93.94
XRF (ppm)													
Sc	3	2	3	3	2	4	2	3	3	3	2	3	3
V	2	1											3
Cr	2	1	1	2	1	3	1	5	3	1	2	4	3
Ni	0	0											0
Cu	0	1	4	4	6	8	4	10	1	5	5	3	2
Zn	41	34	43	49	31	39	33	41	44	45	47	37	38
Ga	15	15	16	17	17	19	18	18	15	16	17	17	17
Rb	159	150		149	149	150	159	156	161	147	151	157	118
Sr	51	54	99	88	71	71	54	55	43	54	52	84	50
Y	15	15	18	19	24	21	18	17	20	19	20	21	29
Zr	102	107	105	100	102	108	104	105	104	104	109	104	126
Nb	11.3	11.4	16	13	14	13	15	13	14	15	15	13	13.2
La	40	41	51	44	55	54	49	33	29	39	49	49	51
Ce	62	69	69	62	81	76	80	59	51	65	65	67	82
Nd	21	23											35
Cs	9	5	13	3	4	4	3	2	1	2	3	4	9
Ba	495	511	803	783	743	720	597	589	473	587	624	696	604
Pb	28	29	40	32	25	30	31	26	36	30	29	31	30
Th	20	21	21	23	15	18	21	16	18	22	15	20	24
U	7	5											4
ICP-MS (ppm)													
Sc	2.4	2											2.9
Rb	162.3	151.6											121.3
Sr	51	54											51
Y	15.28	14.21											29.1
Zr	105	109											130
Nb	11.8	12.3											14.09
Cs	8.39	5.47											6.5
Ba	503	531											625
Hf	3.79	3.88											4.55
Ta	1.11	1.17											1.31
Pb	28.63	29.09											30.6
Th	20.53	21.74											23.92
U	7.13	6.53											5.29
La	40.07	44.34											57.44
Ce	69.79	74.31											87.44
Pr	7.57	8.27											10.47
Nd	24.67	26.72											36.66
Sm	4.11	4.37											6.45
Eu	0.41	0.46											0.95
Gd	2.94	3.06											5.72
Tb	0.45	0.45											0.87
Dy	2.65	2.6											5.12
Ho	0.54	0.51											1.01
Er	1.53	1.4											2.75
Tm	0.24	0.22											0.41
Yb	1.62	1.48											2.6
Lu	0.26	0.24											0.42
Lab	WSU	WSU	SNLL	SNLL	SNLL	SNLL	SNLL	SNLL	SNLL	SNLL	SNLL	SNLL	WSU

(*continued*)

TABLE 1. CHEMICAL ANALYSES OF THE TUFF OF CAMPBELL CREEK AND RELATED ROCKS (*continued*)

	Tuff of Campbell Creek (*continued*)												
Sample	H10-67	H03-116	H03-135	H02-91	H02-90	H01-61	H02-24	H00-10	H08-58	H09-75	CA-31	H09-63	H09-65
Location	Soda Springs	Soda Springs	Kirkwood	Diamond Mts	Diamond Mts	Dogskin Mtn	Dogskin Mtn	Tule Peak	White Rock Canyon	Shoshone Meadows section, Clan Alpine Mts	Shoshone Meadows section, Clan Alpine Mts	Reese River Narrows	Reese River Narrows
Position	base			lower	upper			lower		base		single pumice	single pumice
	vitrophyre	devitrified	devitrified	devitrified	devitrified	devitrified	devitrified	vitrophyre	devitrified	vitrophyre	devitrified	single white pumice	dense white pumice
Latitude	39.28882	39.26878	38.68028	40.1145	40.11455	39.940	39.969	39.922	39.91787	39.78746	39.78675	39.94387	39.94387
Longitude (W)	120.38390	120.37492	120.0623	120.27497	120.2747	119.814	119.840	119.735	118.03166	117.63972	117.63938	117.14153	117.14153
SiO_2	76.78	76.71	76.97	76.96	76.04	76.54	77.05	75.57	75.20	76.92	77.22	75.75	75.91
TiO_2	0.119	0.118	0.109	0.115	0.129	0.138	0.108	0.11	0.109	0.09	0.091	0.097	0.096
Al_2O_3	13.04	13.12	13.04	13.12	13.26	13.12	12.98	13.33	13.37	12.75	12.60	13.19	13.20
FeO*	1.13	0.91	0.76	0.62	1.55	1.20	0.74	0.98	0.85	0.87	0.72	1.06	1.03
MnO	0.03	0.043	0.013	0.024	0.022	0.026	0.012	0.05	0.021	0.06	0.012	0.067	0.058
MgO	0.14	0.12	0.07	0.05	0.15	0.14	0.07	0.41	0.07	0.09	0.11	0.48	0.53
CaO	0.77	0.78	0.56	0.66	0.72	0.74	0.63	0.95	0.49	0.64	0.67	1.18	1.11
Na_2O	2.89	3.45	3.32	3.68	3.33	3.68	3.47	3.35	2.98	3.20	3.43	2.52	2.57
K_2O	5.09	4.73	5.14	4.76	4.76	4.41	4.94	5.22	6.89	5.36	5.13	5.65	5.47
P_2O_5	0.014	0.016	0.012	0.012	0.027	0.016	0.017	0.03	0.015	0.014	0.017	0.012	0.017
LOI									1.19	3.43		5.66	5.33
Total	94.98	94.35	96.56	96.89	96.52	97.24	96.72	96.60	97.72	95.97	96.69	93.54	93.72
XRF (ppm)													
Sc	3	3	2	3	3	3	2		2	3	3	2	3
V	5	5	3	4	6	5	3	8	6	1	7	32	4
Cr	5	2	1	2	2	1	2	5	1	2	1	2	2
Ni	2	0	0	0	0	0	0	18	0	2	0	2	2
Cu	2	0	0	0	0	1	0	3	0	1	0	2	1
Zn	41	47	27	33	46	45	34	46	40	42	37	45	38
Ga	15	14	14	14	15	14	15	17	13	14	15	16	15
Rb	159	147	149	147	149	125	146	154	162	158	158	151	144
Sr	77	85	66	66	89	133	70	99	65	58	62	91	79
Y	15	16	14	12	12	14	15	14	18	16	11	16	15
Zr	109	106	104	107	118	133	107	111	104	104	99	108	108
Nb	11.6	10	10	10.6	10.1	9.6	10.3	12	9.9	11.6	9.1	11.2	11.2
La	34	33	35	37	35	38	40	35	39	37	37	40	33
Ce	64	67	65	60	63	66	70	66	66	66	61	64	65
Nd	23	24	20	23	22	27	24		23	25	21	21	23
Cs	9	8	2	7	6	3	3		0	7	7	8	9
Ba	648	675	634	641	771	1112	621	727	905	540	527	401	487
Pb	28	26	27	26	26	25	26	19	18	30	25	27	27
Th	18	19	20	20	21	18	21	18	22	20	19	21	21
U	6	6	5	6	5	6	7		7	7	5	6	6
ICP-MS (ppm)													
Sc		2.4	1.9	2.3	2.5	2	2.1	5	2.3	2.3	1.9	2	1.9
Rb		150.8	150.8	149.9	150.6	126.3	147.3		164.6	156.5	163.1	150.8	144.6
Sr		86	66	67	89	133	71		65	57	62	89	78
Y		14.88	13.37	11.31	11.64	13.45	15.28		16.36	14.39	10.94	14.85	14.62
Zr		109	108	111	120	136	110		107	103	103	110	109
Nb		10.83	11.05	11.46	11.11	10.22	11.21		11.03	11.25	10.37	11.74	10.91
Cs		7.33	3.86	6.22	5.7	3	4.41		1.24	7.62	6.89	7.19	6.84
Ba		707	648	658	794	1145	633		919	551	548	402	497
Hf		3.76	3.75	3.82	3.96	4.2	3.82		3.61	3.55	3.65	3.68	3.67
Ta		1	1.06	1.06	1.04	0.94	1.03		1.04	1.06	1.07	1.11	1.02
Pb		27.53	27.46	27.24	26.42	26.22	26.5		19.38	28.5	25.44	26.68	25.37
Th		19.16	20.39	20.08	19.54	17.93	20.37		19.21	19.83	19.68	20.79	20.58
U		6.61	4.5	6.03	5.61	5.89	6.65		5.55	6.68	4.1	6.43	6.24
La		39.63	39.12	39.77	37.83	42.32	42.41		39.58	38.99	38.78	38.38	36.71
Ce		67.9	70.73	66.92	66.44	69.17	70.22		69.28	67.55	67.29	67.76	68.57
Pr		7.41	7.26	7.37	7.11	8.32	7.92		7.53	7.31	7.02	7.25	6.91
Nd		24.21	23.27	23.59	22.88	27.88	25.78		24.71	23.48	22.34	23.62	22.17
Sm		4.02	3.77	3.78	3.78	4.53	4.19		4.07	3.88	3.48	3.95	3.71
Eu		0.51	0.44	0.47	0.52	0.72	0.52		0.51	0.41	0.39	0.37	0.35
Gd		2.92	2.58	2.57	2.59	3.12	2.97		2.97	2.85	2.35	2.86	2.73
Tb		0.44	0.38	0.38	0.38	0.45	0.45		0.47	0.43	0.35	0.43	0.41
Dy		2.59	2.26	2.12	2.13	2.57	2.62		2.77	2.51	1.96	2.48	2.46
Ho		0.52	0.45	0.4	0.42	0.5	0.52		0.57	0.51	0.38	0.51	0.5
Er		1.48	1.32	1.08	1.17	1.35	1.46		1.68	1.43	1.09	1.47	1.42
Tm		0.23	0.21	0.17	0.18	0.21	0.22		0.27	0.23	0.18	0.24	0.23
Yb		1.52	1.39	1.13	1.2	1.44	1.45		1.82	1.53	1.19	1.57	1.51
Lu		0.25	0.23	0.18	0.19	0.24	0.23		0.3	0.25	0.2	0.27	0.25
Lab	WSU	WSU	WSU	WSU	WSU	WSU	WSU	WSU	WSU	WSU	WSU	WSU	WSU

(*continued*)

TABLE 1. CHEMICAL ANALYSES OF THE TUFF OF CAMPBELL CREEK AND RELATED ROCKS (*continued*)

	Tuff of Campbell Creek (*continued*)											
Sample	H01-139	H01-140	H09-81	H09-82	06-DJ-26	H07-95	H10-79	H00-101	H08-33	H08-35	H10-101	H11-188
Location	Reese River Narrows	Reese River Narrows	Clipper Gap	Clipper Gap	Caetano caldera	Welches Canyon	E Humboldt Range	Intracaldera	Intracaldera	Intracaldera	Intracaldera	Intracaldera
Position	lower	upper	base	top				lower	middle	upper	in megabreccia	in megabreccia
	vitrophyre	devitrified	vitrophyre	devitrified	vitrophyre	vitrophyre	clay alteration	devitrified	devitrified	devitrified	vitrophyre	vitrophyre
Latitude	39.94438	39.94438	39.22224	39.22296	40.21064	40.81077	41.04334522	39.24111	39.25480	39.26357	39.21527	39.45571
Longitude (W)	117.14159	117.14159	116.85332	116.85322	117.01116	116.29791	115.0673571	117.65833	117.67982	117.72656	117.69030	117.64095
SiO_2	76.23	76.77	76.55	76.52	76.89	75.12	77.76	77.36	76.78	77.40	75.96	76.80
TiO_2	0.103	0.103	0.094	0.101	0.113	0.112	0.113	0.096	0.119	0.101	0.134	0.08
Al_2O_3	13.15	12.76	12.81	12.68	12.83	13.66	13.67	12.67	13.13	13.10	13.13	12.33
FeO*	1.06	1.01	1.01	1.07	0.79	1.08	1.07	1.02	1.09	1.08	1.26	1.52
MnO	0.051	0.051	0.069	0.042	0.017	0.046	0.017	0.012	0.015	0.039	0.073	0.07
MgO	0.26	0.07	0.08	0.07	0.07	1.55	1.78	0.19	0.17	0.24	0.21	0.09
CaO	0.79	0.71	0.67	0.63	0.69	1.22	2.24	0.63	0.80	1.49	1.06	0.65
Na_2O	3.19	3.69	3.26	3.68	3.67	2.05	0.33	3.16	3.07	2.08	4.00	3.61
K_2O	5.15	4.82	5.44	5.19	4.90	5.15	2.99	4.85	4.81	4.45	4.14	4.84
P_2O_5	0.015	0.012	0.015	0.018	0.023	0.022	0.022	0.018	0.024	0.031	0.029	<0.01
LOI			2.84	0.95								3.50
Total	93.86	97.67	96.57	98.58	98.77	90.28	89.39	95.77	96.81	96.51	94.68	98.70
XRF (ppm)												
Sc	2	3	2	2	3	1	3	3	3	3	2	
V	3	1	3	7	13	7	5	2	4	8	10	
Cr	1	1	3	3	1	2	4	1	2	2	5	
Ni	0	0	1	2	5	0	3	0	0	0	2	
Cu	1	0	1	1	1	0	2	0	0	0	3	18
Zn	78	35	43	44	27	42	39	39	43	46	44	56
Ga	14	14	15	15	16	15	13	15	15	16	15	16.2
Rb	145	147	154	152	158	128	49	154	150	147	202	
Sr	80	67	68	64	78	99	4029	60	90	105	116	
Y	14	15	16	14	11	16	13	14	14	15	16	
Zr	104	106	107	110	112	109	103	98	114	82	111	
Nb	10.8	10.6	11.2	11.7	9.9	11.5	13.2	10.4	11.1	8.9	11.4	
La	37	38	36	39	38	36	36	35	39	30	37	
Ce	60	66	63	66	64	70	61	65	66	54	65	
Nd	21	22	25	24	19	24	20	22	25	20	23	
Cs	9	5	6	2	7	11	2	7	2	5	16	
Ba	659	685	662	573	693	442	8108	521	644	932	557	
Pb	34	29	30	29	26	27	15	26	22	18	28	
Th	19	20	19	20	19	21	21	19	20	18	20	
U	6	5	7	5	6	6	4	4	7	5	5	
ICP-MS (ppm)												
Sc	2	2	2.4	2.4		2.4		1.9		2.6		
Rb	149	145.1	155	152.1		133.2		157.2		147.8		173
Sr	83	66	68	63		103		60		107		58.3
Y	14.5	13.83	14.37	12.63		15.39		13.93		12.97		14.3
Zr	108	106	109	110		111		103		83		106
Nb	11.17	10.35	11.16	11.38		12.2		11.49		9.76		12.2
Cs	7.02	5.63	7.52	4.92		6.97		5.29		4.3		7.46
Ba	689	679	680	583		462		544		932		545
Hf	3.79	3.69	3.59	3.78		3.93		3.66		3		3.8
Ta	1.06	0.99	1.04	1.09		1.1		1.07		0.96		1.2
Pb	36.37	28.07	27.87	26.73		28.48		26.92		19.06		36
Th	20.02	19.58	19.4	20.18		21.06		20.55		17.76		21.8
U	6.53	5.24	6.46	5.24		5.44		5.56		4.71		6.47
La	40.6	39.46	39.51	39.67		41.12		39.14		30.92		40.6
Ce	65.88	65.92	68.41	67.11		73.61		67.13		55.47		71.9
Pr	7.5	7.34	7.26	7.56		7.71		7.25		6.17		7.80
Nd	24.33	23.89	23.68	24.64		25.05		23.24		20.45		24.0
Sm	4.01	3.93	3.85	4.14		4.12		3.76		3.74		3.88
Eu	0.48	0.49	0.46	0.46		0.43		0.43		0.57		0.40
Gd	2.86	2.8	2.8	2.95		3.04		2.69		2.82		2.70
Tb	0.43	0.42	0.42	0.43		0.46		0.4		0.42		0.39
Dy	2.54	2.44	2.53	2.4		2.68		2.37		2.31		2.35
Ho	0.5	0.48	0.5	0.46		0.53		0.47		0.44		0.47
Er	1.44	1.37	1.41	1.24		1.52		1.41		1.23		1.47
Tm	0.23	0.22	0.23	0.19		0.24		0.23		0.18		0.22
Yb	1.52	1.46	1.49	1.27		1.63		1.54		1.19		1.62
Lu	0.25	0.24	0.25	0.2		0.27		0.25		0.19		0.25
Lab	WSU	WSU	WSU	WSU	WSU	WSU	WSU	WSU	WSU	WSU	WSU	ALS

(*continued*)

TABLE 1. CHEMICAL ANALYSES OF THE TUFF OF CAMPBELL CREEK AND RELATED ROCKS (*continued*)

	Tuff of Campbell Creek (*continued*)			Intrusive rocks of Campbell Creek caldera			Tuff E					
Sample	H11-189	H11-190	H11-6	H10-97	H10-93	H10-104	22–1B	HP-X	H99-29	H00-57	H01-78	C05-695
Location	Intracaldera	Intracaldera	Intracaldera	Intracaldera	Intracaldera	Intracaldera	Haskell	Haskell Peak	Soda Springs	Sand Springs Range	Wassuk Range	Flowery Peak
Position	north	north	dacite pumice	dacite dome	rhyolite band	anorthoclase dike	base		base	base		base
	devitrified	devitrified	devitrified	devitrified	devitrified	devitrified	vitrophyre	devitrified	vitrophyre	vitrophyre	devitrified	vitrophyre
Latitude	39.45815	39.45783	39.24110	39.29058	39.30674	39.27991		39.67459	39.2675	39.04283	38.97555	39.36963
Longitude (W)	117.65129	117.65201	117.65868	117.62185	117.62806	117.70256		120.56226	120.37133	118.3675	119.02316	119.51968
SiO_2	76.56	76.59	70.70	66.16	76.86	70.73	73.71	74.19	76.02	76.59	76.91	76.75
TiO_2	0.10	0.09	0.26	0.505	0.127	0.406	0.10	0.138	0.125	0.11	0.092	0.112
Al_2O_3	12.42	12.38	15.53	17.43	12.70	15.57	15.50	14.64	13.89	12.88	12.69	13.08
FeO*	1.58	1.72	2.70	3.51	1.10	2.19	2.32	2.09	0.92	1.12	1.04	0.80
MnO	0.07	0.07	0.05	0.068	0.033	0.016	0.03	0.019	0.025	0.035	0.008	0.058
MgO	0.17	0.07	0.61	0.70	0.16	0.26	0.46	0.19	0.11	0.09	0.17	0.11
CaO	0.78	0.62	1.49	3.12	0.70	0.68	1.41	1.22	1.07	0.73	0.75	0.71
Na_2O	3.50	3.86	4.30	4.63	3.42	4.26	1.86	2.52	2.66	3.72	2.87	3.68
K_2O	4.82	4.61	4.25	3.69	4.88	5.81	4.50	4.97	5.17	4.69	5.42	4.69
P_2O_5	<0.01	<0.01	0.11	0.19	0.03	0.083	0.08	0.015	0.012	0.026	0.052	0.017
LOI	1.50	1.10	2.00									3.22
Total	99.60	99.90	99.40	97.79	97.50	96.64		93.90	93.84	97.80	97.44	98.49
XRF (ppm)												
Sc				4	3	9	3	4	3	2	3	3
V				42	9	3		10	5	4	10	3
Cr				6	6	2	2	5	6	4	5	3
Ni				3	2	2		3	4	3	2	0
Cu	18	19	18	3	2	1	6	9	2	8	3	2
Zn	69	60	102	72	32	90	38	31	26	42	25	43
Ga	16.2	16.5	19.4	19	16	21	15	15	15	15	14	15
Rb				91	154	135	130	138	141	137	186	150
Sr				668	247	19	221	193	153	80	88	78
Y				11	16	25	19	17	14	12	14	16
Zr				278	112	314	115	118	110	114	76	106
Nb				8.8	12.2	16.6	10	9.1	8.8	11.5	10.4	11
La				36	40	42	43	35	38	43	25	39
Ce				65	66	84	61	56	64	68	45	64
Nd				23	25	35		22	21	23	19	22
Cs				1	6	2	6	11	11	8	7	
Ba				2386	648	1980	1600	1545	1350	709	536	660
Pb				20	24	27	35	25	27	28	27	28
Th				9	21	14	24	23	27	19	28	20
U				3	4	6		9	8	5	10	9
ICP-MS (ppm)												
Sc												
Rb	176	176	133									
Sr	91.1	58.5	343									
Y	14.2	15.1	13.0									
Zr	111	110	305									
Nb	11.8	12.6	8.8									
Cs	5.96	7.13	5.76									
Ba	756	556	3950									
Hf	3.9	3.8	7.2									
Ta	1.2	1.2	0.7									
Pb	25	40	26									
Th	21.2	22.5	11.7									
U	4.51	6.37	3.98									
La	41.8	42.6	34.1									
Ce	70.4	73.4	59.8									
Pr	8.07	8.15	6.75									
Nd	25.2	25.2	22.3									
Sm	4.08	4.12	3.74									
Eu	0.45	0.41	1.14									
Gd	2.74	2.87	2.60									
Tb	0.40	0.42	0.36									
Dy	2.32	2.52	2.13									
Ho	0.47	0.51	0.44									
Er	1.42	1.55	1.28									
Tm	0.23	0.24	0.20									
Yb	1.54	1.74	1.46									
Lu	0.24	0.26	0.23									
Lab	ALS	ALS	ALS	WSU	WSU	WSU	SNLL	WSU XRF	WSU XRF	WSU XRF	WSU XRF	

Note: LOI—loss on ignition. WSU—X-ray fluorescence (XRF) and inductively coupled plasma-mass spectrometry (ICP-MS) at Geoanalytical Lab, Washington State University; SNLL— X-ray fluorescence at Sandia National Laboratory, Livermore, California, USA. ALS—ICP-atomic emission spectrometry and ICP-MS at ALS Minerals. ll analyses normalized to 100% anhydrous. FeO*–total Fe reported as FeO. Sum–total before normalization to 100% anhydrous.

TABLE 2. $^{40}Ar/^{39}Ar$ SANIDINE AGES AND PHENOCRYST ABUNDANCES OF THE TUFF OF CAMPBELL CREEK AND RELATED ROCKS.

Sample	Tuff (or Dated Unit)	Location	State	Age (Ma)	± 2σ	K/Ca	± 1σ	n*	Latitude	Longitude	Phenocrysts (%) Total	Plag	San	Qtz	Biot	Hbl	Px
	Postcollapse rocks of Campbell Creek caldera																
H10-104	Anorthoclase rhyolite dike	Southern part of caldera	NV	25.26	0.09	6.0	2.0	6/6	39.27991	–117.70256	3	3			tr		
H10-93	Rhyolite of Dacite-Rhyolite domes	Eastern part of caldera	NV	28.84	0.05	54.7	3.4	11/23	39.30674	–117.62806	8	4	2	1	1		
H10-97	Dacite of Dacite-Rhyolite domes	Eastern part of caldera	NV	28.83	0.04	55.4	6.3	15/21	39.29058	–117.62185	40	30	5	1	3	1	
	Tuff of Campbell Creek																
HP-3B	distal welded, devitrified	Haskell Peak, eastern Sierra Nevada	CA	28.86	0.05	NM	NM	15/15	39.67459	–120.56212	4	2	1	1	tr		
H02-90	upper cooling unit	Black Mtn, Diamond Mts	CA	28.86	0.09	53.7	8.3	15/15	40.11455	–120.27470	7	3	2	1	<1		
H02-91	lower cooling unit	Black Mtn, Diamond Mts	CA	28.98	0.08	52.8	8.1	10/10	40.11450	–120.27497	8	3	2	2	1		
H03-135	distal welded, devitrified	Carson Pass, eastern Sierra Nevada	CA	28.99	0.07	57.2	8.5	14/15	38.68028	–120.06230	6	2.5	1.5	1.5	0.5		
H02-24	distal welded, devitrified	Dogskin Mtn	NV	29.04	0.10	59.6	6.6	15/15	39.96883	–119.84000	6	2	1.5	1.5	0.5	tr	tr
H01-61	distal welded, devitrified	Dogskin Mtn	NV	29.04	0.06	57.5	5.8	16/16	39.94000	–119.81433	7	2	2	3	<1		
NH07-043	distal welded, devitrified	Lee-Allen hot springs	NV	28.73	0.10	54.8	5.7	15/15	39.24841	–118.73182	10	2	4	3	<1		
H01-139	basal vitrophyre	Reese River Narrows, Shoshone Range	NV	28.84	0.09	55.4	13.3	10/10	39.94438	–117.14159	10	4	3	2	1		
H10-101	intracaldera vitrophyre in megabreccia	southern Desatoya Mts	NV	28.95	0.07	54.1	7.1	4/6	39.21527	–117.69030	8	4	2	1	0.5	0.2	0.5
H00-101	intracaldera, stratigraphically lowest exposed	Campbell Creek, Desatoya Mts	NV	28.99	0.07	49.1	6.3	11/11	39.24111	–117.65833	9	4	2	2	1		
CA-1	distal welded, devitrified	Deep Canyon, Clan Alpine Mts	NV	28.98	0.11	55.2	3.5	8/8	39.65783	–117.87067	8	3	2	2	1		
H09-82	base, upper cooling unit	Clipper Gap, Toquima Range	NV	28.92	0.08	55.0	3.5	12/14	39.22296	–116.85322	8	2	3	3	tr		
H09-81	basal vitrophyre, lower cooling unit	Clipper Gap, Toquima Range	NV	28.92	0.06	54.2	4.4	10/15	39.22224	–116.85332	10	4	2	4	tr	tr	tr
Wallace	distal nonwelded	Welches Canyon, Tuscarora Mts	NV	28.99					40.81077	–116.29791	4	1.5	1	1	tr	tr	
H10-79	distal nonwelded	East Humboldt Range	NV	28.93	0.07	54.5	5.6	16/19	41.04335	–115.06736	7	2	3	2	tr		
Mean				28.934	0.071	28.956	0.062	without sample NH07-043									
	Tuff E																
HP-X	distal welded, devitrified	Haskell Peak, eastern Sierra Nevada	CA	29.22	0.04	NM	NM	15/15	39.67459	–120.56226	15	7	3	4	1	tr	tr
H99-29	distal welded, vitrophyre	Soda Springs, eastern Sierra Nevada	CA	29.21	0.08	72.1	10.2	15/15	39.26750	–120.37133	10	3	3	3	1		
C05-695	distal welded, vitrophyre	Flowery Peak, Virginia Range	NV	29.17	0.07	55.8	20.0	14/14	39.36963	–119.51968	12	3	5	3	tr	tr	tr
F06-454	distal welded, devitrified	Painted Rock, Virginia Range	NV	29.21	0.04	71.3	18.8	15/15	39.60172	–119.35684	20	7	7	4	2		alt?
H01-78	distal welded, devitrified	Wassuk Range	NV	29.21	0.06	88.2	31.7	15/15	38.97555	–119.02316	22	5	7	8	1		alt?
H00-57	basal vitrophyre	Sand Springs Range	NV	29.11	0.07	60.6	12.1	12/12	39.04283	–118.36750	7	4	1	2	<1		
Mean				29.188	0.042												
GSCN 200	unnamed tuff	Cactus Range, Nellis Test Range	NV	20.32	0.04	NM	NM	14/15	37.731	–116.805	43	8	12	20	3		
H01-136	unnamed tuff	Shoshone Mtns, Gold Park	NV	24.72	0.05	46.8	18.4	15/15	39.14883	–117.54517	20	2	10	8	tr	tr	
H00-88	tuff of Desatoya Peak	Pony Canyon, Desatoya Mts	NV	24.74	0.06	51.2	5.7	15/15	39.38694	–117.80194	25	12	5	3	3	1	<1
H00-86	tuff of Railroad Ridge (Eureka Canyon?)	South Fork War Canyon, Clan Alpine Range	NV	25.15	0.06	53.7	4.6	15/15	39.58333	–117.86000	25	12	8	5	2	alt?	

Note: Sanidine was separated from crushed, sieved samples by standard magnetic and density techniques, leached with dilute HF to remove matrix, and handpicked.

All analyses except Wallace at New Mexico Geochronological Research Laboratory, New Mexico Institute of Mining and Technology. Analytical methods in McIntosh et al. (2003).

Weighted mean $^{40}Ar/^{39}Ar$ ages of sanidine from individual samples calculated by the method of Samson and Alexander (1987). Samples were irradiated in Al discs for 7 hours in D-3 position, Nuclear Science Center, College Station, Texas, USA. Neutron flux monitor Fish Canyon Tuff sanidine (FC-1); assigned age = 28.201 Ma (Renne and others, 1998; Kuiper et al. 2008).

Decay constants and isotopic abundances after Steiger and Jäger (1977); lb = 4.963×10^{-10} yr^{-1}; le+e′ = 0.581×10^{-10} yr^{-1}; $^{40}K/K = 1.167 \times 10^{-4}$

Wallace: 2007 written commun. from Alan R. Wallace, analysis at U.S. Geological Survey, Menlo Park.

Mt–Mountain; Mts–Mountains. Plag–plagioclase; San–sanidine; Qtz–quartz; Biot–biotite; Hbl–hornblende; Px–pyroxene; tr–trace; alt–altered; NV—Nevada; CA—California.

*Number (n) of single grains used in age calculation/total number of sanidine grains analyzed.

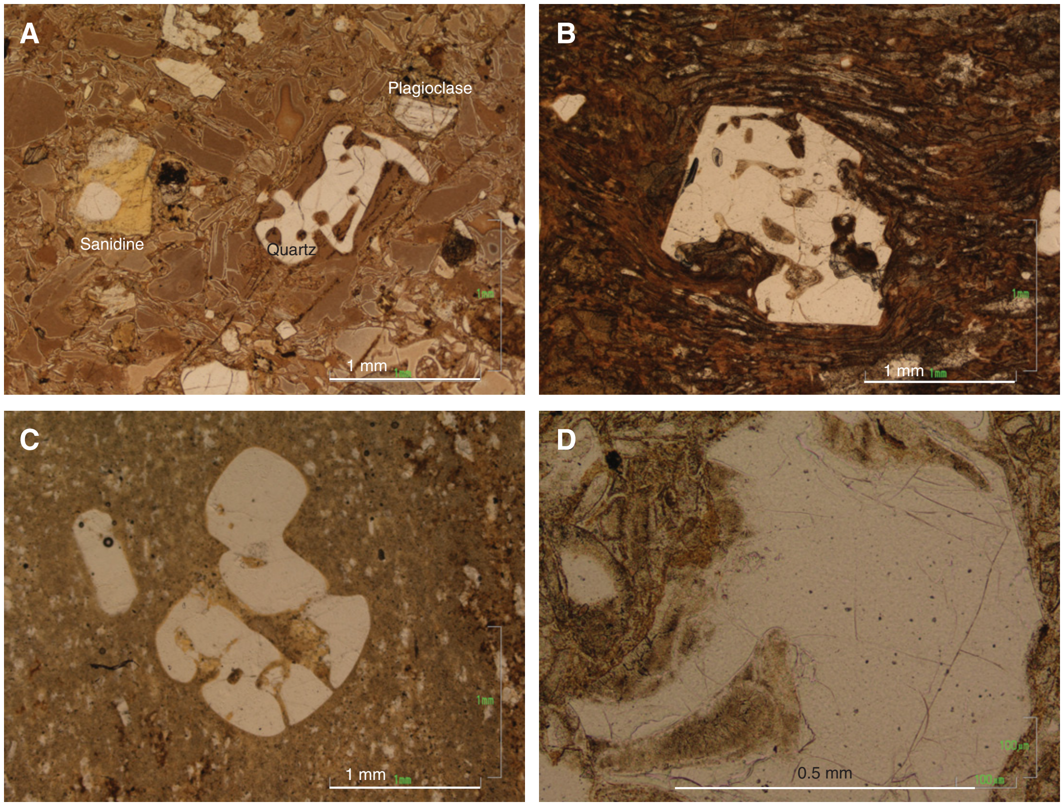

Figure 4. Representative photomicrographs of tuff of Campbell Creek showing characteristic vermicular (resorbed) quartz phenocrysts and large glass shards. (A) Intracaldera vitrophyre, Desatoya Mountains (H10-101). (B) Thick devitrified tuff, Clan Alpine Mountains (CA-31). (C) Rhyolite band in dacite dome in caldera, Desatoya Mountains (H10-93). (D) Thin poorly welded tuff, East Humboldt Range, most eastern known location (H10-79).

preserve pyramidal shape. The similarity of the two tuffs means that tuff E may not have been recognized in areas where a cooling break between the two tuffs is poorly exposed. Tuff E probably represents an early eruption from the Campbell Creek caldera in the Desatoya Mountains (Brooks et al., 2008). It has not been positively identified in or near the caldera, although an older tuff that makes up part of the caldera wall may be tuff E (Fig. 6). A postcaldera rhyolite contains sparse, possibly xenocrystic sanidine grains that give ages indistinguishable from that of tuff E.

Sanidine $^{40}Ar/^{39}Ar$ ages of 12 samples of tuff of Campbell Creek that span its distribution vary between 29.04 ± 0.10 and 28.84 ± 0.09 Ma, with one anomalously low age from a hydrothermally altered sample at 28.73 ± 0.10 Ma (Table 2; all $^{40}Ar/^{39}Ar$ ages discussed in this paper were calculated or recalculated to an age of 28.201 Ma for Fish Canyon Tuff sanidine; Kuiper et al., 2008). K/Ca clusters tightly ca. 55 Ma (range 49.1 ± 6.3–59.6 ± 6.6). Sanidine $^{40}Ar/^{39}Ar$ ages of 6 samples of tuff E range from 29.22 ± 0.06–29.11 ± 0.07 Ma. K/Ca varies from 55.8 ± 20.0–88.2 ± 31.7, higher and more variable than in the tuff of Campbell Creek.

The tuff of Campbell Creek also has a relatively distinctive characteristic remanent magnetization (CHRM), which can be used to test possible correlations. For example, CHRMs from 10 paleomagnetic sites in the Diamond and Fort Sage Mountains in northeastern California and westernmost Nevada, respectively, yield a group mean of 206.1° (declination) and –43.0° (inclination) for the tuff of Campbell Creek (Fig. 7A; Hinz et al., 2009). Because vertical-axis rotation is negligible in this area, this mean can serve as a reference direction for the tuff of Campbell Creek. In central Nevada, the C unit of the Bates Mountain Tuff has a nearly identical CHRM (Fig. 7B). The group mean of the CHRM from six sites in the Bates Mountain C Tuff (203.6° declination and –44.1° inclination; Gromme et al., 1972; Hudson and Geissman, 1991) overlaps the reference direction of the tuff of Campbell Creek at the 95% confidence level (Fig. 7C), supporting correlation of the two tuffs.

Our age, composition, petrographic, and paleomagnetic data demonstrate that the tuff of Campbell Creek is the same as the C unit of the Bates Mountain Tuff of central Nevada. The Bates Mountain Tuff was defined to consist of several individual ash-flow tuffs at Bates Mountain (Fig. 1; McKee, 1968; Stewart and McKee, 1968; Sargent and McKee, 1969). Subsequent stratigraphic subdivision, based in part on paleomagnetic data, recognized four ash-flow cooling units, A–D, and showed the C unit to be present at Clipper Gap and Reese River Narrows (Gromme et al., 1972). Our work shows that the C units at those two locations and at the type locality at Bates Mountain are the same as the tuff of Campbell Creek. The informal name tuff of Campbell Creek is preferred over Bates Mountain Tuff, because the latter consists of four unrelated tuffs, all with informal letter designations.

Caldera Source

Although examined only in reconnaissance for this study, the caldera source for the tuff of Campbell Creek in the Desatoya Mountains is reasonably well established based on the presence of thick intracaldera tuff of Campbell Creek, megabreccia, probable southwestern, southern, and northwestern caldera walls, and post-tuff dacite-rhyolite intrusions (Fig. 6; Barrows, 1971; McKee and Stewart, 1971; Stewart and McKee, 1977; this study). The Desatoya Mountains and Campbell Creek calderas are at most slightly tilted (intracaldera tuff is flat-lying to gently east dipping), so exposure is limited to upper parts of the caldera. In the area of Campbell Creek, intracaldera tuff mostly consists of a single, petrographically homogeneous, densely welded cooling unit >600 m thick; the base is not exposed (Fig. 5G). The uppermost intracaldera tuff consists of poorly welded, lithic tuff interbedded with lenses of conglomerate.

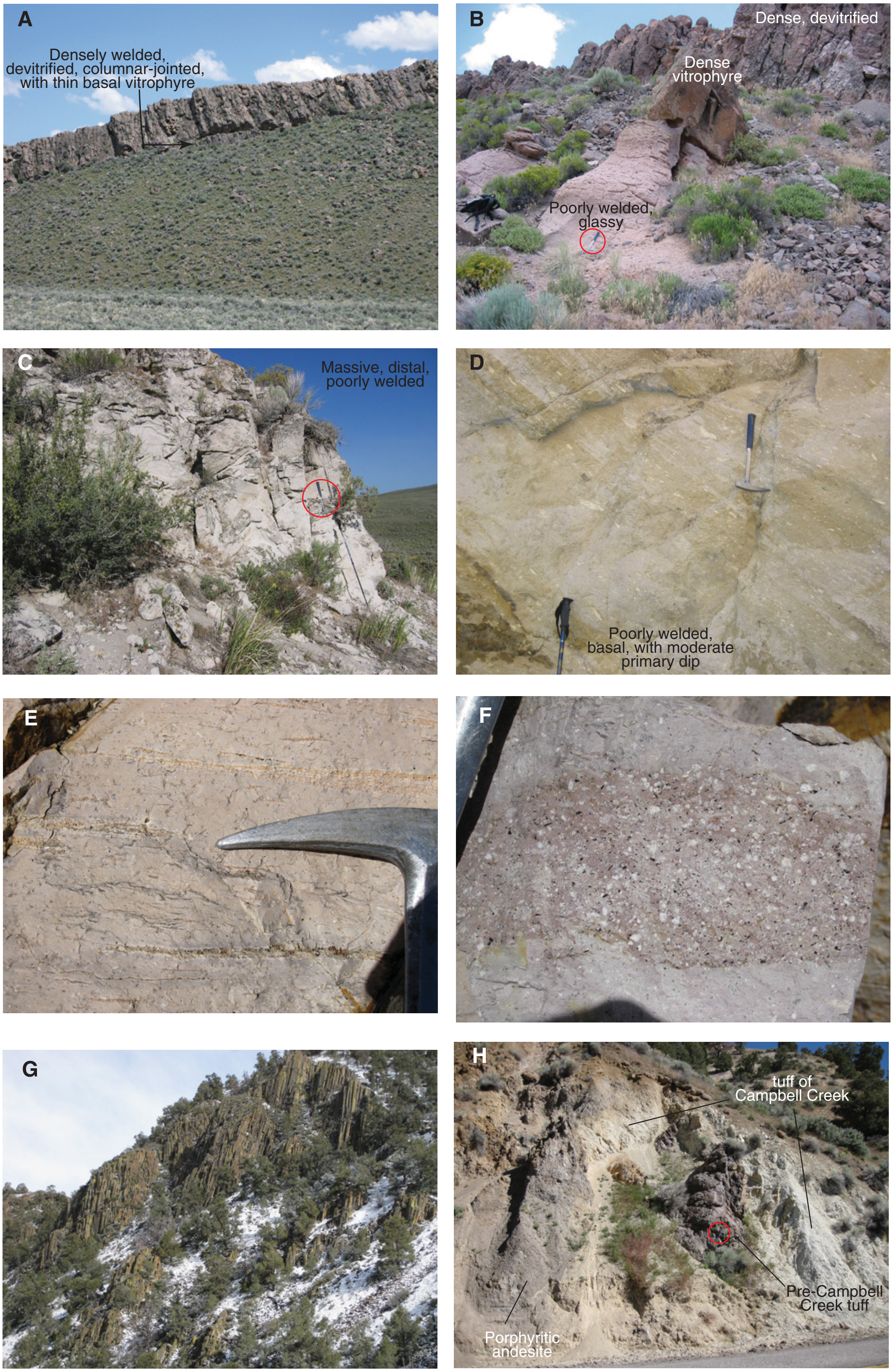

Figure 5. Outcrop characteristics of tuff of Campbell Creek. (A) Typical exposure of outflow tuff in Caetano caldera (Fig. 1). Densely welded, devitrified, columnar-jointed tuff makes an ~8-m-thick resistant ledge with a thin welded basal vitrophyre. Upper, nonwelded tuff probably was deposited but stripped by erosion. (B) Typical section grading from poorly welded, glassy base to densely welded vitrophyre to densely welded devitrified tuff, Reese River Narrows (Fig. 1). Rock hammer (circled) in all photos is 42 cm long. (C) The most distal outflow tuff is poorly welded and vitrophyric throughout (Welches Canyon; Fig. 1). (D) Distal outflow tuff in canyon of Little Truckee River, Sierra Nevada (Fig. 1), showing ~40° primary dip where tuff compacted against steep slope developed in older ash-flow tuff in a paleovalley. (E) Densely welded intracaldera tuff with slightly stretched pumice, Desatoya Mountains (H00-101 location; Fig. 6). (F) Abundantly porphyritic dacite pumice fragments ~7 cm thick in intracaldera tuff, Desatoya Mountains (H00-101 location; Fig. 6). (G) Typical, thick, densely welded, columnar-jointed intracaldera tuff, Desatoya Mountains ~1.5 km west of location H00-101 (Fig. 6). (H) Megabreccia blocks of porphyritic andesite (left) and older ash-flow tuff (right) in moderately welded intracaldera tuff, southwest margin of caldera (Fig. 6).

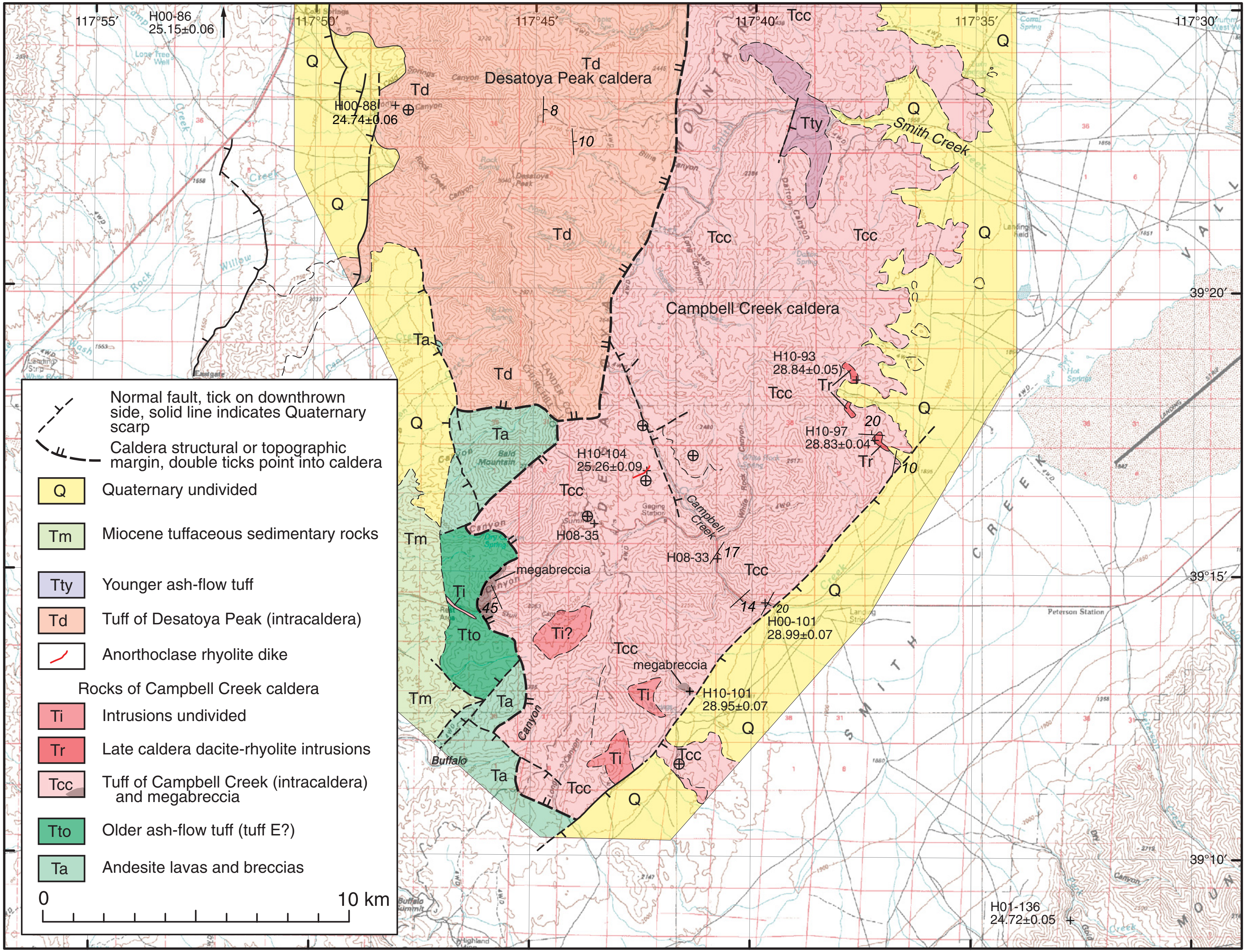

Figure 6. Reconnaissance geologic map of the southern part of the Campbell Creek caldera in the Desatoya Mountains, central Nevada. Geology from Barrows (1971), Stewart and McKee (1977), McKee and Conrad (1987), and this study.

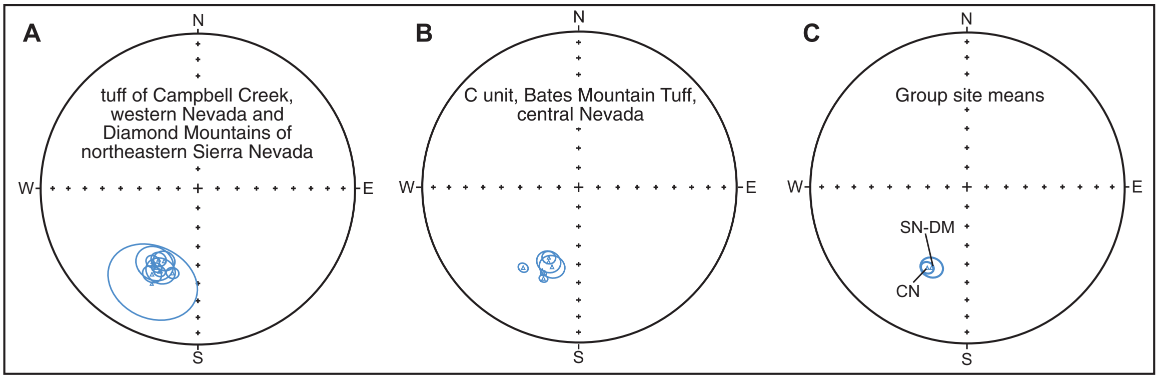

Figure 7. Equal-area projections of site and group mean directions (triangles as projected on the upper hemisphere, reverse polarity) and their 95% confidence cones from paleomagnetic sites of the tuff of Campbell Creek and C unit of the Bates Mountain Tuff. Tilt corrections were applied where applicable. (A) Ten sites from the tuff of Campbell Creek in the Diamond and Fort Sage Mountains of northeastern California and westernmost Nevada, respectively (data from Hinz et al., 2009). The Diamond Mountains are essentially part of the Sierra Nevada. (B) Six sites from the C unit of the Bates Mountain Tuff in central Nevada, including the Clan Alpine Mountains, Shoshone Range, and Toquima Range (data from Gromme et al., 1972; Hudson and Geissman, 1991). (C) Group site means for the tuff of Campbell Creek in the Diamond Mountains region (SN-DM) and C unit of the Bates Mountain Tuff in central Nevada (CN). These means overlap at the 95% confidence level. Combined with other similar features, the paleomagnetic data indicate that the tuff of Campbell Creek and the C unit of the Bates Mountain Tuff are the same ash-flow deposit.

The most densely welded parts are slightly rheomorphic, with stretched pumice fragments as much as 60 cm long and 2 cm thick (Fig. 5E). Megabreccia consisting of blocks of the older ash-flow tuff or porphyritic andesite as much as 20 m across surrounded by vitrophyric tuff of Campbell Creek is present near the probable southwestern, southern, and northwestern margins of the caldera (Figs. 5H and 6).

Several intrusions are mapped in the caldera, although we have examined only the composite dacite-rhyolite intrusions (unit Tr; Fig. 6). Most of the observed dacite-rhyolite intrusive rock is coarsely and abundantly porphyritic dacite (H10-97; 66% SiO_2; Table 1) that is petrographically and compositionally more like the dacite pumice than the rhyolitic tuff of Campbell Creek. Dacite intrusions contain 40% phenocrysts, mostly plagioclase, with lesser sanidine, biotite, minor vermicular quartz, and sparse hornblende. The dacite intrusions are even less evolved than the dacite pumice, with higher TiO_2, Al_2O_3, FeO, MgO, CaO, Sr, Zr, and Ba abundances and lower K_2O, Rb, Nb, Th, and U abundances than the tuff of Campbell Creek. Bands of rhyolite (H10-93; 77% SiO_2) in dacite in the northern outcrop area are petrographically and compositionally indistinguishable from the tuff. They contain <10% phenocrysts of subequal amounts of plagioclase, sanidine, and highly vermicular quartz, and minor biotite. Major and trace elements show the same abundances as the tuff (Figs. 2 and 3). Sanidine $^{40}Ar/^{39}Ar$ ages from a rhyolite and a dacite are 28.84 ± 0.05 and 28.83 ± 0.04 Ma, overlapping with the age of the tuff of Campbell Creek (Table 2). The age and location of the dacite-rhyolite intrusions, the similarity of the rhyolite part to the main tuff of Campbell Creek, and the similarity of the dacite part to the dacite pumice are strong evidence that all are genetically related. Rhyolite bands are almost certainly residual (nonerupted) tuff of Campbell Creek magma. Dacite is probably additional residual but less silicic magma that provides further evidence for a compositionally variable magma chamber. The two residual magma components partly mixed during emplacement of the dacite-rhyolite intrusions. The sparse dacite pumice in intracaldera tuff indicates minor mixing during initial ash-flow eruption.

The younger, ca. 24.7 Ma Desatoya Peak caldera cuts out the western part of the Campbell Creek caldera (Fig. 6; Table 2). Probable outflow tuff of Desatoya Peak crops out in the Shoshone Mountains southeast of the Campbell Creek caldera. The tuff of Desatoya Peak contains 20%–25% phenocrysts of plagioclase, sanidine, quartz, biotite, and minor hornblende and clinopyroxene and orthopyroxene (Table 2). An anorthoclase-phyric dike that intrudes intracaldera tuff of Campbell Creek is significantly younger (25.26 ± 0.09 Ma; H10-104; Table 2), but older than the tuff of Desatoya Peak, and compositionally distinct from Campbell Creek rocks (Fig. 2).

We estimate the area of the Campbell Creek caldera to be ~600 km^2, and total volume of erupted tuff to be between 1200 and 3000 km^3. Uncertainty about the location of the caldera margin in several places and total thickness of intracaldera tuff preclude more precise estimates (Figs. 1 and 6). The caldera is at least 35 km north-south from a well-located caldera margin near Buffalo Canyon to the northern part of the Desatoya Mountains, where intracaldera tuff is at least 400 m thick and contains abundant megabreccia. The east-west dimension is at least 14 km and probably closer to 20 km, but is poorly known because the younger Desatoya Peak caldera and basin-and-range faults cut off the Campbell Creek caldera to the west and east.

Estimating the volume of intracaldera outflow, or total erupted tuff is even more uncertain. Flow and deposition of the tuff of Campbell Creek in paleovalleys make estimates of outflow tuff especially difficult. We find that total erupted volume is best approximated from the volume of caldera collapse where it is known (John et al., 2008a; Henry and Faulds, 2010). Assuming 2–5 km of collapse, which is representative of calderas in Nevada, erupted volume could range from 1200 to 3000 km^3. Even the lower value makes the tuff of Campbell Creek and caldera a supereruption and supervolcano (Mason et al., 2004; Sparks et al., 2005; Miller and Wark, 2008), which is consistent with the wide distribution of the tuff.

Distribution

The tuff of Campbell Creek is distributed across an area of at least 55,000 km^2 from the western foothills of the Sierra Nevada east to the East Humboldt Range (northern Ruby Mountains). Notably, the tuff is found ~100 km east of our interpreted Oligocene drainage divide in east-central Nevada (Fig. 1; Henry, 2008), or even farther east of the alternative divide of Best et al. (2009). The present-day west-southwest–east-northeast extent, parallel to paleovalleys through that region, is ~530 km. The tuff reached a distance from its source caldera to the west of at least 200 km, corrected for later extension using the values of Henry and Faulds (2010), and ~215 km to the northeast, based on estimated extension of Colgan and Henry (2009). The actual flow distance would have been greater in each direction because the paleovalleys were not straight and because known outcrops probably do not represent the greatest original extent. As with other outflow tuffs in western and central Nevada, thickness correlates poorly with distance from source.

The distribution of the tuff of Campbell Creek is distinctive compared to that of other tuffs that erupted in the western part of the central Nevada caldera belt that also flowed long distances down the west-draining paleovalleys (Henry and Faulds, 2010). (1) It spread much farther east, upstream in the paleovalleys, even across the interpreted paleodivide, whereas other tuffs commonly traveled only ~60 km upstream. (2) Its north-northwest extent, perpendicular to the trend of the paleovalleys, is significantly greater, ~160 km, than the perpendicular extent of other tuffs, <~100 km. The tuff flowed until ~100 km to the north and ~60 km to the south, crossing several east-west divides between major paleovalleys. (3) The tuff flowed in at least five major paleovalleys in western Nevada and the eastern Sierra Nevada, whereas most tuffs were restricted to one or two major paleovalleys. Only the Nine Hill Tuff, which spread similar distances to the west, almost as far to the northeast, and farther east to near Ely, Nevada, from a possible source in the Carson Sink, has a similar or greater distribution among tuffs of the Great Basin (Deino, 1989; Best et al., 1989). The Peach Springs Tuff in southern Nevada and northwestern Arizona also flowed northeastward across the probable paleodivide (see Regional Orogenic Highland discussion).

Why did the tuff of Campbell Creek travel so much farther than other tuffs from the central Nevada caldera belt? Particularly, how was it able to flow upstream across the inferred major north-south paleodivide and to cross several divides between west-draining paleovalleys near the source (Fig. 1)? The occurrences at Welches Canyon and the East Humboldt Range are particularly problematic because they are so far from the caldera, "upstream" from the source, and across several inferred east-west drainage divides. No single factor seems capable of generating such wide distribution, and each factor has its drawbacks. (1) Large eruptive volume seems essential, and the possible 3000 km^3 volume makes the tuff of Campbell Creek one of the most voluminous eruptions of the central Nevada caldera belt (Best et al., 1989, 1995; Mason et al., 2004). However, other voluminous tuffs are not so extensive. Both the ~1100 km^3 Caetano Tuff and ~1200–1600 km^3 lower tuff of Mount Jefferson are largely restricted to single paleovalleys (John et al., 2008a; Henry and Faulds, 2010). (2) The tuff of Campbell Creek may have had distinctive magmatic and eruptive characteristics that contributed to wider distribution. For example, it may have been hotter and had a higher eruption column than most other tuffs, although we have no direct evidence for either. The Nine Hill Tuff, which has a similar wide distribution, is sparsely porphyritic and moderately alkalic (but neither it nor the tuff of Campbell Creek are peralkaline); was hot, with magmatic temperatures of 850–930 °C (Deino, 1985); and is commonly highly rheomorphic. These features are contributors to or indicators of low viscosity and wide distribution. The tuff of Campbell Creek has the same features except for high magmatic temperature, which is unknown. A high eruption column would give the tuff the potential and then kinetic energy from column collapse to surmount significant topography. We have no information on eruption dynamics for either tuff, but suggest that the similarities between them indicate their wide distributions arise in part from similar causes. (3) Intervalley relief may have been especially low when the tuff of Campbell Creek erupted. The 28.9 Ma tuff of Campbell Creek erupted at the end of a nearly continuous, 2.5 Ma (31.4–28.9 Ma) period of voluminous ash-flow eruptions (Faulds et al., 2005) from calderas in the Stillwater Range–Clan Alpine Mountains–Desatoya Mountains region. Pyroclastic material from preceding eruptions at least partly filled topography close to the Campbell Creek caldera, which reduced intravalley relief and probably made it easier for the tuff to disperse more widely.

Factors external to the tuff of Campbell Creek, such as location of the paleodivide or gradients across the Nevadaplano, could also influence distribution but would apply to other tuffs erupted from the central Nevada caldera belt, which did not flow as far. Two interpretations depict paleotopography of the Nevadaplano very differently (Fig. 8). (1) Based on stable isotope studies, Cassel et al. (2010, 2012a) interpreted that the Oligocene Sierra Nevada had an elevation and steep gradient similar to its present-day elevation and gradient, and that the Nevadaplano east about to the Campbell Creek caldera had a much shallower gradient. A shallow gradient in the central Nevadaplano would have allowed the tuff of Campbell Creek, as well as any other tuff, to flow more easily upstream. In contrast, Best et al. (2009) used an analogy to the Andean Altiplano to interpret that the Nevadaplano had a nearly constant gradient to a paleodivide at ~4 km elevation slightly west of where we place it, and a nearly flat interior only slightly lower than the paleodivide to the

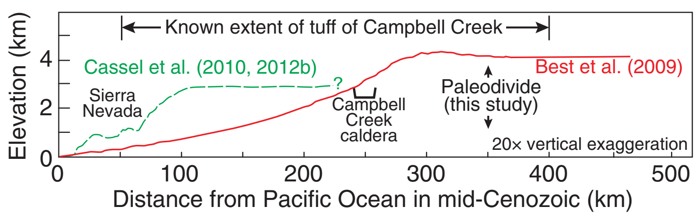

Figure 8. Proposed paleotopography across the Sierra Nevada and Great Basin in relation to the Campbell Creek caldera and distribution of the tuff of Campbell Creek. Paleotopography of Best et al. (2009) requires that the tuff of Campbell Creek flowed upstream ~50 km to crest a paleodivide ~1 km higher than the caldera. However, the Peach Springs Tuff of southern Nevada and northwestern Arizona may also have flowed uphill over the paleodivide in that area (see Regional Orogenic Highland discussion). Paleotopography of Cassel et al. (2010, 2012b), if extrapolated eastward, allows easier eastward flow of the tuff of Campbell Creek but suggests that many other tuffs should also extend far to the east. The elevation of the paleodivide of this study is unknown.

east. The steep western slope would have made it particularly difficult for any tuff to flow to the east and makes the distributions of the tuff of Campbell Creek, Nine Hill Tuff, and possibly Peach Springs Tuff even more problematic. (2) Intervalley relief may have been less near the paleodivide than to the west. Paleovalleys in western Nevada and eastern California were 380–1200 m deep (Proffett and Proffett, 1976; Brooks et al., 2003; Henry, 2008; Henry and Faulds, 2010). Paleovalleys are not as well exposed or examined in the central Nevada caldera belt, but, where exposed, they are >300 to >1000 m deep (this study; John et al., 2008a; Gonsior and Dilles, 2008). The Caetano Tuff, the caldera of which is much closer to our proposed paleodivide, spread almost entirely west of its source caldera (John et al., 2008a).

IMPLICATIONS OF FAR-TRAVELED TUFFS

Structural Evolution of Northern Nevada and the Sierra Nevada

Regardless of how they did so, the pyroclastic flows that deposited the tuff of Campbell Creek and several other 31.4–23.3 Ma ash-flow tuffs flowed great distances from sources in central Nevada through western Nevada and the Sierra Nevada, and other, mostly Eocene tuffs spread over great distances in northeastern Nevada (Fig. 1; Faulds et al., 2005; Henry, 2008; Hinz et al., 2009; Henry and Faulds, 2010). Their ability to flow great distances down paleovalleys across what are now highly faulted Basin and Range and Walker Lane structural provinces confirms the observation of Henry and Faulds (2010) that major faulting postdated ca. 23 Ma. That these tuffs and paleovalleys crossed what is now the Basin and Range–Sierra Nevada structural and topographic boundary further confirms that the Sierra Nevada was topographically lower than what is now the Basin and Range, regardless of the absolute elevations of either (Mulch et al., 2006; Cassel et al., 2009a; Henry and Faulds, 2010).

The fact that the tuff of Campbell Creek reached the East Humboldt Range places significant limits on the amount of pre–29 Ma extension across north-central Nevada to the Ruby Mountains–East Humboldt Range metamorphic core complex. Different studies have concluded markedly different amounts of pre–29 Ma extension in and around the core complex. Abundant thermochronologic and thermobarometric data indicate that the core complex underwent ~170 °C of cooling and 4 kbar of decompression between ca. 85 and ca. 50 Ma, and another 450 °C cooling and 4–5 kbar decompression between ca. 50 and ca. 21 Ma, which requires a total of ~30 km of exhumation (McGrew and Snee, 1994; Snoke et al., 1997; McGrew et al., 2000; Henry et al., 2011). If accomplished by surface-breaking extension, that amount of exhumation would have greatly uplifted the Ruby Mountains and probably generated major basin-and-range topography around them. In contrast, studies of paleovalleys, mapped normal faults in northeast Nevada, and thermochronology of the southern Ruby Mountains indicate a minor episode of extension ca. 40 Ma and major extension after ca. 17 Ma (Henry, 2008; Colgan and Henry, 2009; Colgan et al., 2010).

The tuff of Campbell Creek crops out in the hanging wall of the west-dipping Ruby Mountains detachment fault, so the tuff would have been farther east relative to the core complex before fault displacement. However, ash flows could not have reached that far east if the Ruby Mountains had been a high range with adjacent low basins at the time. We conclude that either all exhumation and extension in the Ruby Mountains postdated 29 Ma (Colgan et al., 2010), or exhumation was accomplished by a process that did not affect the surface, such as diapirism balanced by adjacent downflow (Howard, 2003; Colgan, 2011; Henry et al., 2011).

The distribution of the 760 ka Bishop Tuff around the Long Valley caldera (Bailey, 1989; McConnell et al., 1995; Hildreth and Wilson, 2007) illustrates well the influence of Basin and Range topography on the flow distance and resulting distribution of a tuff (Fig. 1). With an estimated eruptive volume of ~600–750 km^3, the Bishop Tuff is similar to many mid-Cenozoic tuffs in Nevada. The Bishop Tuff surmounted a ridge only a few hundred meters higher than the western topographic rim of the Long Valley caldera and flowed at least 14 km down the 3–4-km-wide Middle Fork of the San Joaquin River. The tuff spread more radially into three wide (≥20 km) basins to the north, east, and southeast. In each case, the Bishop ash flows spread out, made broad, sheet-like deposits, and traveled much shorter distances than did the channelized mid-Cenozoic tuffs. Maximum flow distance was ~50 km into the northern part of Owens Valley southeast of Long Valley (Bailey, 1989).

Paleotopography of the Nevadaplano

Paleovalley Morphology

Several characteristics of paleovalleys suggest that they resulted from prolonged erosion, possibly aided by the warm, wet Eocene climate (Zachos et al., 2001; Kelly et al., 2005). (1) Although the oldest dated paleovalley-filling tuffs in central and western Nevada are ca. 34 and 31 Ma, the Eocene auriferous gravels that fill the bottoms of paleovalleys in the Sierra Nevada are ca. 52–50 Ma, based on paleoflora evidence (MacGinitie, 1941; Wing and Greenwood, 1993). In the Central Valley of California, the intertidal-deltaic equivalent of the auriferous gravels is the Middle Eocene (Lutetian) ca. 49–40 Ma Ione Formation (Creely and Force, 2007). Low-temperature thermochronology from the Sierra Nevada indicates rapid cooling and interpreted rapid exhumation between ca. 90 and 60 Ma, recording erosion following batholith emplacement, and slower cooling and exhumation after 60 Ma (Cecil et al., 2006; see also House et al., 1997). Therefore, the Sierra Nevada and western Nevada paleovalleys existed by at least 50 Ma and possibly as early as 60 Ma. Paleovalley-filling tuffs in northeastern Nevada are as old as 45 Ma (Henry, 2008), and one underlying gravel is dated as 46 Ma (Haynes, 2003), so the northeastern paleovalleys could be as old as those in the Sierra Nevada. Wing and Greenwood (1993, p. 246) cited 50–52 Ma as the "peak of Cenozoic warmth," and the paleovalleys were almost certainly being eroded at that time. Paleovalleys in Idaho existed by the Late Cretaceous (Janecke et al., 2000; Chetel et al., 2011), although they need not have formed at the same time as the drainages in Nevada. Preservation of deposits as old as 45–52 Ma in the bottoms of the paleovalleys indicates that they had been cut to their full depth by that time and did not deepen significantly before filling with Oligocene ash-flow tuffs.

(2) Paleovalleys were much wider (5–8 km) than they were deep (0.5–1.2 km), commonly with nearly flat bottoms and steep walls (Fig. 9), in strong contrast to the v-shaped canyons of the modern Sierra Nevada. These characteristics are exceptionally well illustrated by a three-dimensional view of the paleovalley at Black Mountain in the northern Sierra Nevada (Fig. 9B; see also Hinz et al., 2009), where intravalley relief was mostly developed on resistant rocks, e.g., metavolcanic rocks at Black Mountain. Interfluves were relatively flat (Fig. 9A; see also Slemmons, 1953). Paleovalleys in Idaho were also much wider than deep (Janecke et al., 2000).

(3) A paleoweathered zone as much as 30 m thick is common, especially in biotite-rich granitic rocks, throughout the distribution of paleovalleys. Weathering of the granitic rocks and of vitrophyric parts of ash-flow tuffs produced smectite. In the Sierra Nevada, vitrophyric parts of tuffs also have weathered to smectite (California Geological Survey, 2009) but, where more intensely weathered in the western Sierra Nevada, underlying granitic rocks are altered to kaolinite (Allen, 1929; Wood, 1994; Creely and Force, 2007). Kaolinite has not been found

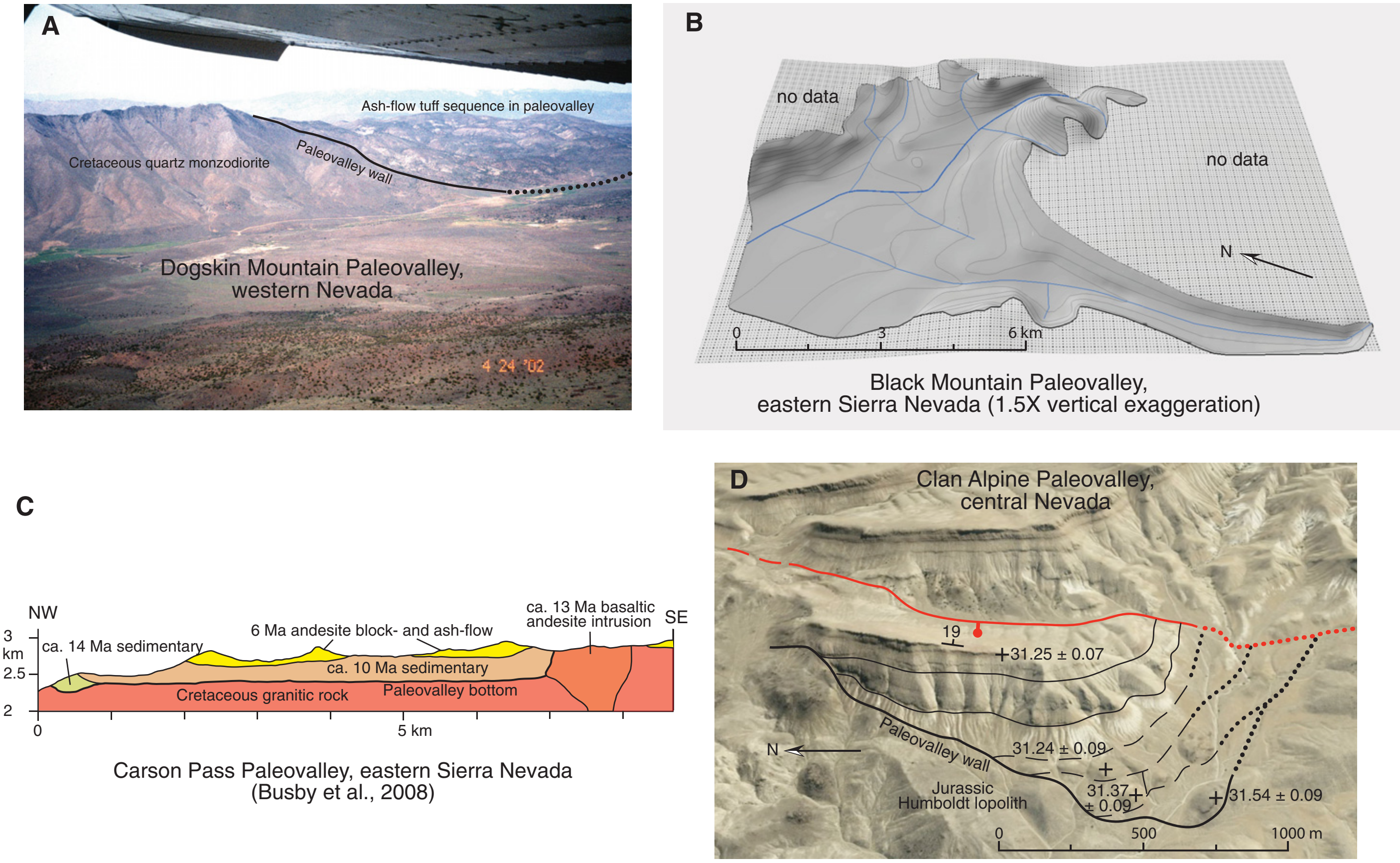

Figure 9. Illustrations of paleovalley morphology; locations in Figure 1. (A) Oblique westward view of paleovalley-filling tuffs and moderately steep paleovalley margin at Dogskin Mountain in western Nevada. Low-relief top of quartz monzodiorite is probably inherited from the Oligocene interfluve. (B) Oblique northeastward view of the paleovalley at Black Mountain in the northern Sierra Nevada that illustrates the flat bottom and steep margins characteristic of paleovalleys. High-relief narrows in the eastern part are underlain by Jurassic(?) metavolcanic rocks; Cretaceous granodiorite underlies the rest of the area. Based on geologic mapping and contouring of base of paleovalley (Hinz et al., 2009). (C) Northwest-southeast cross section of paleovalley at Carson Pass in the central Sierra Nevada (Busby et al., 2008) illustrating that flat bottom persisted into the Middle or Late Miocene. Oligocene ash-flow tuffs crop out in the paleovalley just east of the section. (D) Oblique eastward Google Earth image of paleovalley in the Clan Alpine Mountains of central Nevada. Exposed part of paleovalley was ~350 m deep. Individual tuffs truncate against paleovalley wall of Jurassic Humboldt lopolith.

in the granitic rocks of Nevada. The different mineralogy could indicate either a spatial or temporal change in weathering characteristics. The absence of kaolinite, long recognized as forming by intense leaching in tropical climates (Wilson, 1999), could indicate higher elevation, lower temperature, and less precipitation in Nevada compared to the Sierra Nevada. However, weathering of granitic rocks to smectite can only be demonstrated to have occurred by ca. 31 Ma, the age of the oldest tuffs overlying smectite-weathered granitic rocks in Nevada. Therefore, the mineralogical change could indicate a change in climate over time, with less intense weathering during the cooler, dryer Oligocene compared to the Eocene. Berner and Kothavala (2001) showed a significant decrease in atmospheric CO_2 ca. 50 Ma that might have caused a drop in pCO_2 in soil moisture, higher pH, and less intense weathering. A temporal change might suggest that Eocene weathering in Nevada generated kaolinite, but none of it is preserved, which seems unlikely.

Absolute Elevation

Isotopic and paleobotanical data are interpreted to record a Nevadaplano and eastern, high part of what is now the Sierra Nevada as high as 3 km in the middle Cenozoic (Fig. 8; Wolfe et al., 1997; Horton and Chamberlain, 2006; Mulch et al., 2006; Crowley et al., 2008; Cassel et al., 2009a, 2009b, 2010; Hren et al., 2010), although Molnar (2010) contested the significance of the isotopic data. Based on estimates of crustal thickness and analogy to the Altiplano of the Andes, Best et al. (2009) interpreted a paleodivide at an elevation of ~4 km. In contrast, erosion and river incision data from the Sierra Nevada are interpreted to indicate that it underwent 1.5–2.5 km of uplift in the latest Cenozoic from much lower elevations in the middle Cenozoic (Wakabayashi and Sawyer, 2001; Jones et al., 2004; Stock et al., 2004). The distribution of mid-Cenozoic ash-flow tuffs demonstrates that the Sierra Nevada was a western ramp to the former Nevadaplano, but do not quantitatively indicate paleoelevation. That the tuffs commonly flowed as much as 200 km from source, much farther than most other documented ash-flow tuffs of the world (Cas and Wright, 1987), in channels carrying coarse boulders (Henry, 2008; Henry and Faulds, 2010; Cassel and Graham, 2011), suggests the rivers had moderately steep gradients.

However, the record of two far-traveled Quaternary ash-flow tuffs where the present-day topography is essentially unchanged since the time of eruption suggests that steep gradients are not required. The >60 km^3, 70% SiO_2, 90 ka Aso-4I1 tuff of Kyushu, Japan, flowed as much as 125 km to the sea from a caldera with a rim elevation of between 800 and 1200 m (Matumoto, 1943; Lipman, 1967; Kaneko et al., 2007), a topographic gradient of ~8 m/km. The Morrinsville ignimbrite in New Zealand is interpreted to have flowed ~200 km to the sea from a caldera near Taupo (~500 m elevation; Walker and Wilson, 1983), a gradient of only 2.5 m/km. Unfortunately, very little is published about the Morrinsville ignimbrite, including composition or tuff volume, and Walker and Wilson (1983, p. 131) stated that distal parts of the tuff "cease to have the characters normally regarded as typical of ignimbrites."

Although neither the Aso tuff nor Morrinsville ignimbrite are ideal analogs for the mid-Cenozoic ash-flow tuffs, they demonstrate that an ignimbrite need not erupt from a caldera at high elevation to flow a long distance. A minimum gradient of 2.5 m/km would require paleovalley bottoms in the region of source calderas in central Nevada (200–300 km from the Oligocene coastline) to have been at altitudes of ~500 m. With 300–1000-m-deep paleovalleys, interfluves would have reached elevations of ~1500 m. The distribution of ash-flow tuffs in paleovalleys therefore allows but does not require high mid-Cenozoic elevations in central Nevada.

DID PALEOVALLEYS CROSS THE SOUTHERN SIERRA NEVADA?

Although well-known paleovalley systems crossed the northern and central Sierra Nevada, only one paleovalley is known to have crossed the southern Sierra Nevada south of Sonora Pass (Figs. 1 and 10). Huber (1981, p. 3) documented an ancestral San Joaquin River that "headed at least as far east as the present Mono Lake basin, possibly farther north or east in Nevada." The valley of this ancestral San Joaquin River was much wider than deep (as much as 10 km by 450–750 m) and drained into the Eocene Ione Formation at the edge of the Great Valley. The oldest preserved deposits in the ancestral San Joaquin paleovalley are Late Miocene gravels containing 11 Ma pumice, which Huber (1981) interpreted to be derived from a similar-age tuff east of Mono Lake. The 10 Ma trachyandesite of Kennedy Table filled the paleovalley. Oligocene ash-flow tuffs or other pre–10 Ma deposits may be absent because they were never deposited in the ancestral San Joaquin River valley (source calderas in central Nevada were farther away), or because they were not preserved; few Miocene volcanic rocks were deposited that could have capped and preserved older deposits.

Neither paleovalley deposits nor the mid-Cenozoic landscape are preserved south of the ancestral San Joaquin River, but geologic data from the Death Valley region, southern Sierra Nevada, and San Joaquin Basin allow the existence of several trans-Sierra drainages. Eocene to Early Miocene tuff-bearing sedimentary sequences are common in the Death Valley, California, to Yucca Mountain, Nevada, region (Fig. 10). These deposits were termed Tertiary older sedimentary rocks (Barnes et al., 1982; Slate et al., 2000), the Amargosa Valley Formation (Cemen et al., 1999), and the Titus Canyon and Ubehebe Formations (Snow and Lux, 1999) in different areas. These sedimentary sequences are as much as 800 m thick and generally consist of a coarse basal conglomerate, overlain by mixed clastic rocks and freshwater limestone (Cemen et al., 1999; Snow and Lux, 1999). Dates determined for interbedded tuffs in these deposits are (1) 34 Ma in the basal conglomerate and 30 Ma higher in the Titus Canyon Formation (Saylor and Hodges, 1994), (2) 30 Ma on pyroclastic-fall tuff interbedded with argillaceous limestone in the Tertiary older sedimentary rocks (Barnes et al., 1982; Slate et al., 2000), (3) 25–20 Ma on tuffs (mostly pyroclastic-fall deposits) in the Amargosa Valley Formation (Cemen et al., 1999), and (4) 24.0, 23.0, and 20.3 Ma on ash-flow tuffs in the Ubehebe Formation (Snow and Lux, 1999; their $^{40}Ar/^{39}Ar$ ages recalculated to a monitor age equivalent to 28.201 Ma on Fish Canyon Tuff sanidine). Farther south in Nevada, west-flowing streams deposited gravels containing rounded quartzite boulders in the Late Oligocene or Early Miocene; the gravels are overlain by Middle Miocene ash-flow tuffs derived from the east (Fig. 10; Kohl, 1978; Hanson, 2008).

The tectonic environment of these mid-Cenozoic sedimentary and volcanic rocks is uncertain. Major extension in the Death Valley area began no earlier than ca. 16 Ma, but the existence of earlier extension is debated. Snow and Lux (1999), Snow and Wernicke (2000), and Niemi (2002) interpreted these deposits to have accumulated in ca. 36 and 25 Ma extensional basins, whereas Cemen et al. (1999) interpreted deposition in a broad floodplain but discounted any pre–Middle Miocene extension. Bedding in pre-Cenozoic rocks, Eocene to Early Miocene rocks, and basal parts of definitely Middle Miocene synextensional deposits is concordant (Cemen et al., 1999; Snow and Lux, 1999), which indicates that no measurable tilting, and presumably extension, occurred before the Middle Miocene. Pre–Middle Miocene sedimentary deposits in the Lake Mead area also preceded major extension beginning ca. 17 Ma (e.g., Lamb et al., 2011; Umhoefer et al., 2011).

We suggest that the deposits described here could have been deposited in paleovalleys that drained from the northeast and crossed what is now the southern Sierra Nevada. Barnes et al. (1982) specifically interpreted gravels to have been deposited by streams sourced to the north

Figure 10 (*on following page*). Satellite image of southern Nevada and adjacent regions showing alternative interpretations of paleodrainages and paleodivides through time. The southernmost well-established paleodrainage across the Sierra Nevada is from Huber (1981). Lechler and Niemi (2011) interpreted a Paleocene–Eocene drainage system that flowed southeast along what is now Owens Valley east of the Sierra Nevada, then turned southwest, and did not drain from what is now Nevada. However, we suggest that Eocene–Oligocene deposits recognized in the Death Valley–Yucca Mountain area (Barnes et al., 1982; Saylor and Hodges, 1994; Cemen et al., 1999; Snow and Lux, 1999), although interpreted by some as deposited in extensional basins (Snow and Lux, 1999; Snow and Wernicke, 2000), could be parts of a paleodrainage system that crossed the southern Sierra Nevada and connected with the paleodrainage system of Lechler and Niemi (2011) and/or emptied into the San Joaquin Basin (Nilsen and Clarke, 1975; Bartow and McDougall, 1984; Graham and Olsen, 1988). A post-Sevier, pre-Laramide divide probably trended south into California (Goldstrand, 1992, 1994). Development of the Laramide Kingman uplift (ca.70 Ma or later; Beard et al., 2010) probably shifted the divide northeast through northwestern Arizona, where it stayed at least through the time of the 18.5 Ma Peach Springs Tuff (Young, 1979; Bohannon, 1984; Goldstrand, 1994; Beard, 1996; Spencer et al., 2008). Howard (1996, 2000) interpreted a large paleodrainage system to the southwest, to the Pacific Ocean, that would have been across the divide from these northeast-draining systems. In contrast, Davis et al. (2010) proposed that a Late Paleocene–Early Eocene system drained northeastward from southeastern California to Utah, perpendicular to the drainage of Howard (1996, 2000) and across the post-Laramide divide. A possible resolution is that the Davis et al. (2010) system is partly pre-Laramide. Distribution of Peach Springs Tuff is from Glazner et al. (1986) and Valentine et al. (1989) with interpreted caldera from Ferguson (2008). See text for further discussion.

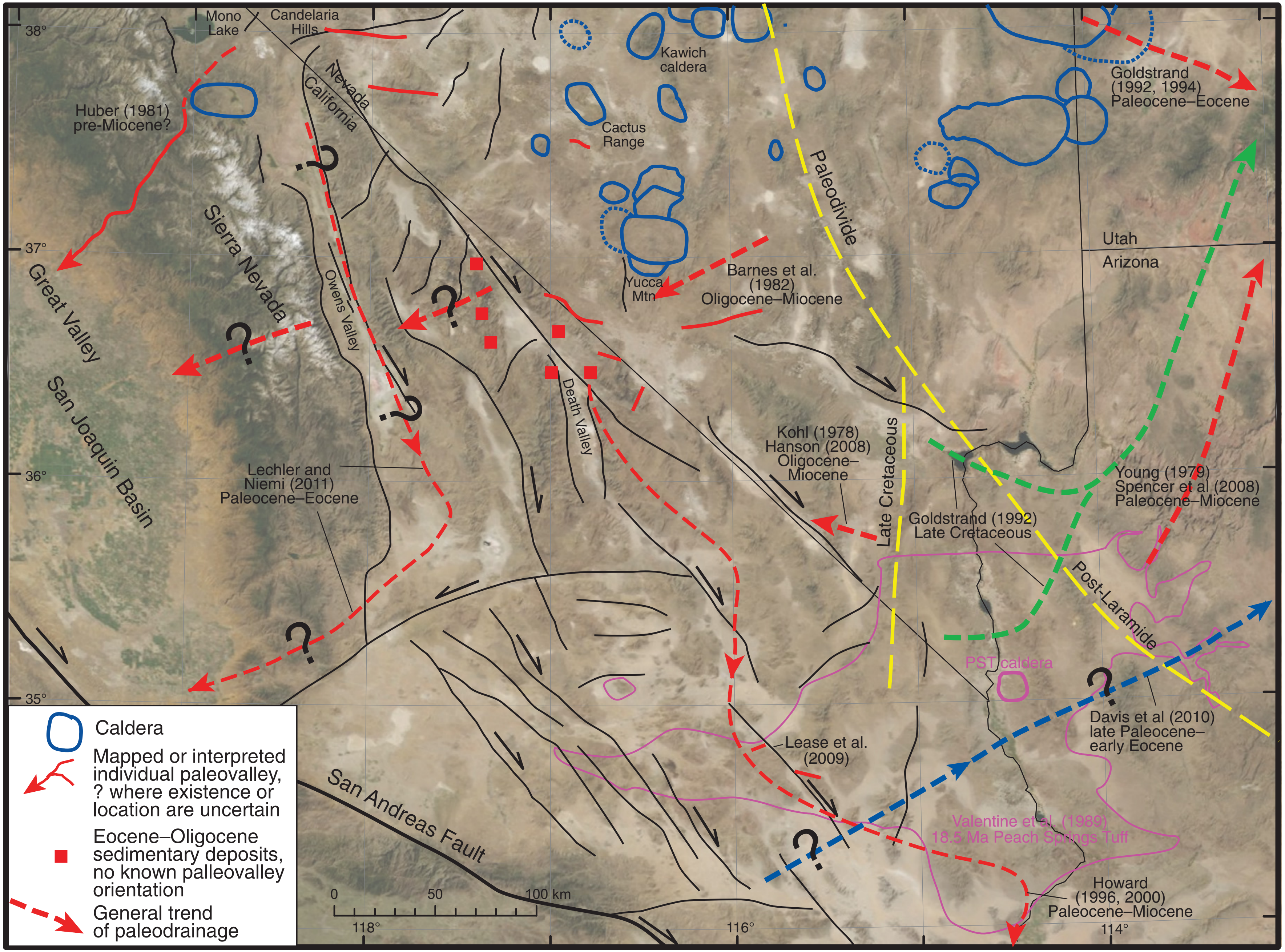

Mono Lake
Candelaria Hills
38°
37°
36°
35°
Kawich caldera
Cactus Range
Huber (1981) pre-Miocene?
Nevada
California
Sierra Nevada
Great Valley
San Joaquin Basin
Owens Valley
Death Valley
Yucca Mtn
Barnes et al. (1982) Oligocene–Miocene
Paleodivide
Goldstrand (1992, 1994) Paleocene–Eocene
Utah
Arizona
Kohl (1978) Hanson (2008) Oligocene–Miocene
Late Cretaceous
Goldstrand (1992) Late Cretaceous
Young (1979) Spencer et al (2008) Paleocene–Miocene
Post-Laramide
Lechler and Niemi (2011) Paleocene–Eocene
PST caldera
Davis et al (2010) late Paleocene–early Eocene
Lease et al. (2009)
Valentine et al. (1989) 18.5 Ma Peach Springs Tuff
Howard (1996, 2000) Paleocene–Miocene
San Andreas Fault
0
50
100 km
118°
116°
114°
Caldera
Mapped or interpreted individual paleovalley, ? where existence or location are uncertain
Eocene–Oligocene sedimentary deposits, no known palleovalley orientation
General trend of paleodrainage

Figure 10.

and northeast, and interbedded tuffs to have come from central and east-central Nevada. Ash-flow tuffs in the Ubehebe Formation are indistinguishable in age from major ash-flow tuffs erupted from the central Nevada caldera belt. Possible correlations include 23.8–24.0 Ma tuffs in the Candelaria Hills (Petronis et al., 2004), the 22.9 Ma Pahranagat Formation erupted from the Kawich caldera (Best et al., 1995; although M.G. Best [2011, written commun.] doubts that the Pahranagat Formation could have traveled that far), and a 20.3 Ma tuff in the Cactus Range (Table 2; Fig. 10). No sources for similar age tuffs exist nearby because the oldest tuffs and calderas of the southwest Nevada volcanic field are ca. 14 Ma (Slate et al., 2000). Based on the distribution of different rock types, Niemi (2002) interpreted the Titus Canyon Formation to have been deposited in a north-northeast–trending extensional basin, which alternatively could have been a north-northeast–trending paleovalley. Except for limestone, the mid-Cenozoic sedimentary and volcanic rocks of the Death Valley–Yucca Mountain region are similar to those filling paleovalleys in western Nevada and the Sierra Nevada (Bateman and Wahrhaftig, 1966; Yeend, 1974; Henry and Faulds, 2010). Eocene paleovalley deposits in northeastern Nevada contain the same rocks and lacustrine limestone (Brooks et al., 1995; Henry, 2008). The mid-Cenozoic rocks around Death Valley must have occupied either throughgoing drainages that crossed what is now the Sierra Nevada or a closed basin of unknown origin.

Two studies of detrital zircon populations in Paleocene–Eocene sedimentary deposits, one in the northern and central and the other in the southern Sierra Nevada, concluded that mid-Cenozoic paleodrainages had headwaters close to or only slightly east of the modern crest of the Sierra Nevada (Cecil et al., 2010; Lechler and Niemi, 2011). Cecil et al. (2010) found predominantly 110–95 Ma and 160–150 Ma detrital zircons in Eocene sedimentary deposits in the northern and central Sierra Nevada, closely coinciding with local batholithic ages. They also found a small subset of pre-Phanerozoic zircons, most abundant in eastern, upstream samples, with age peaks ca. 1800 Ma and 2700 Ma. Cecil et al. (2010) interpreted the pre-Phanerozoic zircons to have been eroded from the early Paleozoic Shoo Fly Complex, which has zircons of similar age and crops out in a range-parallel belt through the western Sierra Nevada (Harding et al., 2000; Spurlin et al., 2000). Similarly, Lechler and Niemi (2011) found predominantly Mesozoic zircons in the Paleogene Goler, Witnet, and Tejon Formations (east to west) in the southern Sierra Nevada, and interpreted the data to indicate a paleodrainage with headwaters restricted to the area of the present Owens Valley (Fig. 10). The deposits also contain a minor population of pre-Mesozoic zircons with age peaks ca. 1800 Ma and 2700 Ma. Lechler and Niemi (2011) dismissed a central Nevada source because of the small proportion of these older zircons, which were 9% in the eastern deposits, 4% in the central deposits, and 2% in the western deposits.

The idea that Eocene drainages in the northern and central Sierra Nevada were sourced no farther east than the modern drainages is incompatible with provenance studies and the distribution of ash-flow tuffs (Bateman and Wahrhaftig, 1966; Yeend, 1974; Faulds et al., 2005; Garside et al., 2005; Cassel et al., 2009a, 2009b, 2012b; Henry and Faulds, 2010; this study). A more extensive study of 1292 detrital zircons in Eocene–Oligocene fluvial sediments in the northern Sierra Nevada (Cassel et al., 2012b) found marked differences in populations (e.g., locally Jurassic-dominated versus mid-Cretaceous dominated) between different sites and 1%–17% Eocene zircons in the Jurassic-dominated populations. In Cassel et al. (2012b), Sierra Nevada drainage patterns are interpreted to have evolved complexly through time, possibly including eastward migration of the paleodivide between the Early and Late Eocene, consistent with possible eastward drainage from northwestern Nevada in the early Cenozoic (van Buer et al., 2009), and definite westward drainage from central Nevada at least by Late Eocene time.

In contrast, the zircon data of Cecil et al. (2010) and Lechler and Niemi (2011) are equally compatible with paleodrainages originating in central Nevada and crossing the Sierra Nevada. Paleogeologic maps of depositional basement to Tertiary rocks in the Sierra Nevada and Basin and Range north of 38°N indicate that Mesozoic plutonic rocks were widely exposed in California and western Nevada, in and east of the modern Sierra Nevada (Van Buer et al., 2009; Cassel et al., 2012b). These batholithic rocks are rich sources of zircons, which, being relatively young and therefore having relatively little radiation damage at the time of erosion and deposition, were robust and underwent only short transport. Regardless of where the headwaters of the paleodrainages were, the Mesozoic batholithic rocks would be expected to contribute the vast majority of zircon to sedimentary rocks on the west side of the Sierra Nevada and would overwhelm any component from farther upstream. In contrast, exposed bedrock in western and central Nevada at this time consisted of Mesozoic and Paleozoic carbonates and deep-water rocks of the Golconda and Roberts Mountains allochthons (mostly chert, argillite, and greenstone), all of which are much poorer sources of zircon than the Mesozoic plutons. However, these rocks contain 1100–2700 Ma zircons (Soreghan and Gehrels, 2000) that were more likely to be metamict and had to undergo at least two cycles of erosion, long-distance transport, and redeposition to be incorporated into Eocene deposits, all of which would tend to wear them down to effectively vanishing (Hay and Dempster, 2009). Eocene sediments in the Sierra Nevada are dominated by Mesozoic zircon because the major source of zircon is the nearby, and underlying, Sierra Nevada batholith. The proportion of older zircons decreases downstream (westward) in both northern and southern Sierra Nevada, consistent with these older zircons being sourced farther east in Nevada, being overwhelmed by the proximal batholithic source of zircon, and possibly being more prone to attrition. Headwaters of the northern and central Sierran drainages have been unequivocally demonstrated to have been in central Nevada by Oligocene time; this suggests that the headwaters for the southern drainages could also have been there. The Eocene–Oligocene deposits of the Death Valley–Yucca Mountain region could have been deposited in the upstream parts of the southern Sierra Nevada drainages (Fig. 10).

Eocene through Miocene sedimentary rocks are widespread in the surface and subsurface of the San Joaquin Basin, along and west of the western edge of the southern Sierra Nevada (Nilsen and Clarke, 1975; Bartow and McDougall, 1984; DeCelles, 1988; Graham and Olsen, 1988; see especially Bent, 1988). All studies call upon an eroding Sierra Nevada as a source; Bartow and McDougall (1984, p. J7) noted the "strong resemblance to the Eocene Ione Formation in its type area 350 km to the northwest," and Nilsen and Clarke (1975) specifically suggested the Great Basin as a source area. Drainages were coming from the southern Sierra Nevada, the only question being the eastern location of their headwaters.

Combining the above data allows two end-member alternatives: (1) the southern Sierra Nevada was a high island in the early through middle Cenozoic and paleodrainages went around it, or (2) paleodrainages crossed the southern Sierra Nevada but both their deposits and geomorphic expression have been removed by erosion. The high island alternative requires that the southern Sierra Nevada underwent distinctly different Late Cretaceous or early Cenozoic evolution than did the northern and central Sierra Nevada. Batholith development was similar along the entire range, especially in the most voluminous Cretaceous phase (Bateman, 1992; Ducea, 2001; Saleeby et al., 2008). However, Saleeby (2003) and Saleeby et al. (2010) interpreted that shallow subduction in the latest Cretaceous–earliest Paleogene removed the lithosphere beneath the southern Sierra Nevada and generated major exhumation, without affecting the Sierra Nevada farther north. The erosional removal alternative requires only that the southern Sierra Nevada be uplifted more than the northern and central Sierra Nevada in the late Cenozoic, consistent with the common interpretation of major latest Cenozoic uplift (1–2 km) resulting from foundering of the eclogitic root of the southern part of the batholith (Ducea and Saleeby, 1998; Farmer et al., 2002; Saleeby et al., 2003; Jones et al., 2004; Zandt et al., 2004; Stock et al., 2004; Figueroa and Knott, 2010). Further examination of the Eocene–Miocene sedimentary rocks in the San Joaquin Basin to identify their source areas would help us to evaluate these alternatives.

REGIONAL OROGENIC HIGHLAND

Combined with other interpreted paleodrainages in Idaho, Oregon, California, Utah, Arizona, and Sonora, Mexico, the data presented in this paper indicate that a late Mesozoic to mid-Cenozoic erosional highland extended from at least central Idaho to northern Sonora (Fig. 11). In Idaho, Janecke et al. (2000) and Chetel et al. (2011) mapped Middle Eocene (ca. 50–47 Ma) paleovalleys (Eocene Idaho River) that drained southeastward from the Sevier thrust belt into the Green River Basin in southwestern Wyoming. West of the paleodivide, several provenance studies indicate drainage from the Idaho batholith west to the Oregon Coast and southwest to northern California (Heller et al., 1985, 1987; Underwood and Bachman, 1986; Renne et al., 1990; Aalto et al., 1998). The southwestern drainage parallels the northwestern edge of the Cretaceous batholith belt, which turns northeast from the Sierra Nevada across northwestern Nevada toward the Idaho batholith (Barton et al., 1988; Lerch et al., 2007; Van Buer et al., 2009). The batholith belt probably was a topographic high in the early Cenozoic that had eastward drainages off its eastern flank (Van Buer et al., 2009). As pointed out by Chetel et al. (2011), the inferred paleodivides in Nevada and Idaho are misaligned by ~200 km; they noted that this misalignment coincides with an interpreted Neoproterozoic transfer zone and major changes in Paleozoic facies (Lund, 2008), where the Roberts Mountains allochthon turns to the northeast in northeastern Nevada after trending north through the rest of Nevada (Stewart, 1980). Greater post-Eocene westward extension in Nevada relative to Idaho probably also contributes to the misalignment.

Considerable data show an orogenic highland through southern Nevada into Arizona (Figs. 10 and 11). Clasts in Late Cretaceous–Paleocene deposits of southern Utah were sourced from the Sevier thrust belt in southern Nevada and eastern California (Goldstrand, 1992; Young, 1979). The pre-Laramide divide probably followed the Sevier thrust belt into eastern California (Goldstrand, 1992). Development of the Laramide Kingman uplift (Bohannon, 1984; Faulds et al., 2001; Beard et al., 2010) probably shifted the divide to the northeast; this beheaded the older drainages (Young, 1979; Bohannon, 1984; Goldstrand, 1994; Beard, 1996). Apatite (U-Th)/He geothermometry data are consistent with major uplift of the southwestern Colorado Plateau following Sevier-Laramide contraction and erosion of 1-km-deep proto–Grand Canyon by the Early Eocene (Flowers et al., 2008). Wernicke (2011) placed this erosion as ca. 80–70 Ma, or following Sevier deformation and preceding the Kingman uplift. The post-Laramide drainage system persisted until extensional faulting began in the Middle Miocene (Bohannon, 1984; Beard, 1996).

The 18.5 Ma Peach Springs Tuff, the youngest major preextensional marker in its region, spread preferentially westward from its caldera source in northwestern Arizona near the borders with Nevada and California (Fig. 10; Glazner et al., 1986; Valentine et al., 1989; Ferguson, 2008). Throughout its distribution, the tuff flowed in paleovalleys, especially where it reached and overtopped the paleodivide to the northeast (Young and Brennan, 1974; Young, 1979; Glazner et al., 1986). The tuff's distribution and flow are similar to those of the Oligocene–Miocene tuffs in western Nevada, although this southern region did not undergo the older volcanism. Notably, the Peach Springs Tuff also flowed upstream and crossed the paleodivide, although the divide was no more than ~50 km east of the caldera. The similarity in early Cenozoic (post-Laramide) and Middle Miocene drainages in northwestern Arizona suggests that the paleodivide maintained its location during that time (Young, 1979).

Interpretations of paleodrainages in southeastern California and northwestern Arizona partly conflict (Figs. 10 and 11). Davis et al. (2010) interpreted that a Late Paleocene–Early Eocene drainage system (California River) extended northeast from southeastern California to northeastern Utah. In contrast, Howard (1996, 2000) interpreted a Late Paleocene–Middle Miocene, ancestral Colorado River that drained southward across southeastern California, perpendicular to and across the drainage of Davis et al. (2010), and then west to the Pacific Ocean (Fig. 11). Lease et al. (2009) found two segments of a generally west-trending paleovalley offset ~24 km by right-lateral faulting in the eastern California shear zone near where the two regional drainages would cross (Fig. 10), but did not identify which way the paleoriver flowed. A possible reconciliation is that detritus in Utah interpreted by Davis et al. (2010) to come from southeastern California did so before formation of the Kingman uplift. Beard et al. (2010) constrained the Kingman uplift to between 70 Ma and Paleocene (65.5–55.8 Ma; Walker and Geissman, 2009), because paleocanyons contain Paleocene deposits. Wernicke (2011) showed the northeastward-draining California River of Davis et al. (2010) being truncated by ca. 55 Ma and the upper reaches of that river becoming parts of an "Arizona River" system that includes the ancestral Colorado River of Howard (1996, 2000) and flowed to the Pacific Ocean.

The southernmost recognized major paleodrainage systems are in southern Arizona and northern Sonora and connect across the San Andreas fault system to Eocene coastal deposits in southern California and northern Baja California (Fig. 11; Abbott and Smith, 1978, 1989; Howard, 1996, 2000). The distribution of these drainages indicates that the paleodivide turned far to the east, following the Laramide belt. Low-temperature thermochronology from the Peninsular Ranges in northern Baja California

Figure 11 (*on following page*). Interpreted synthesis of the regional erosional highland (greater Nevadaplano) from Idaho to Arizona. Paleovalleys in western Nevada and the Sierra Nevada existed at least by ca. 50 Ma based on the age of paleovalley sedimentary deposits and low-temperature thermochronology in California (MacGinitie, 1941; Wing and Greenwood, 1993; House et al., 1997; Cecil et al., 2006; Creely and Force, 2007) and by 45 Ma in northeastern Nevada based on the age of ash-flow tuffs that filled paleovalleys (Henry, 2008). Paleodrainages existed by Late Cretaceous time in Idaho (Janecke et al., 2000) and southern Nevada and Utah (Goldstrand, 1992, 1994) and by Paleocene or Eocene time in Arizona, southern California, and Sonora (Abbott and Smith, 1978, 1989; Young, 1979; Dickinson et al., 1988; Howard, 1996, 2000; Spencer et al., 2008). Laramide uplift in southern Nevada and northwestern Arizona partly deflected the pre-Laramide drainage system.

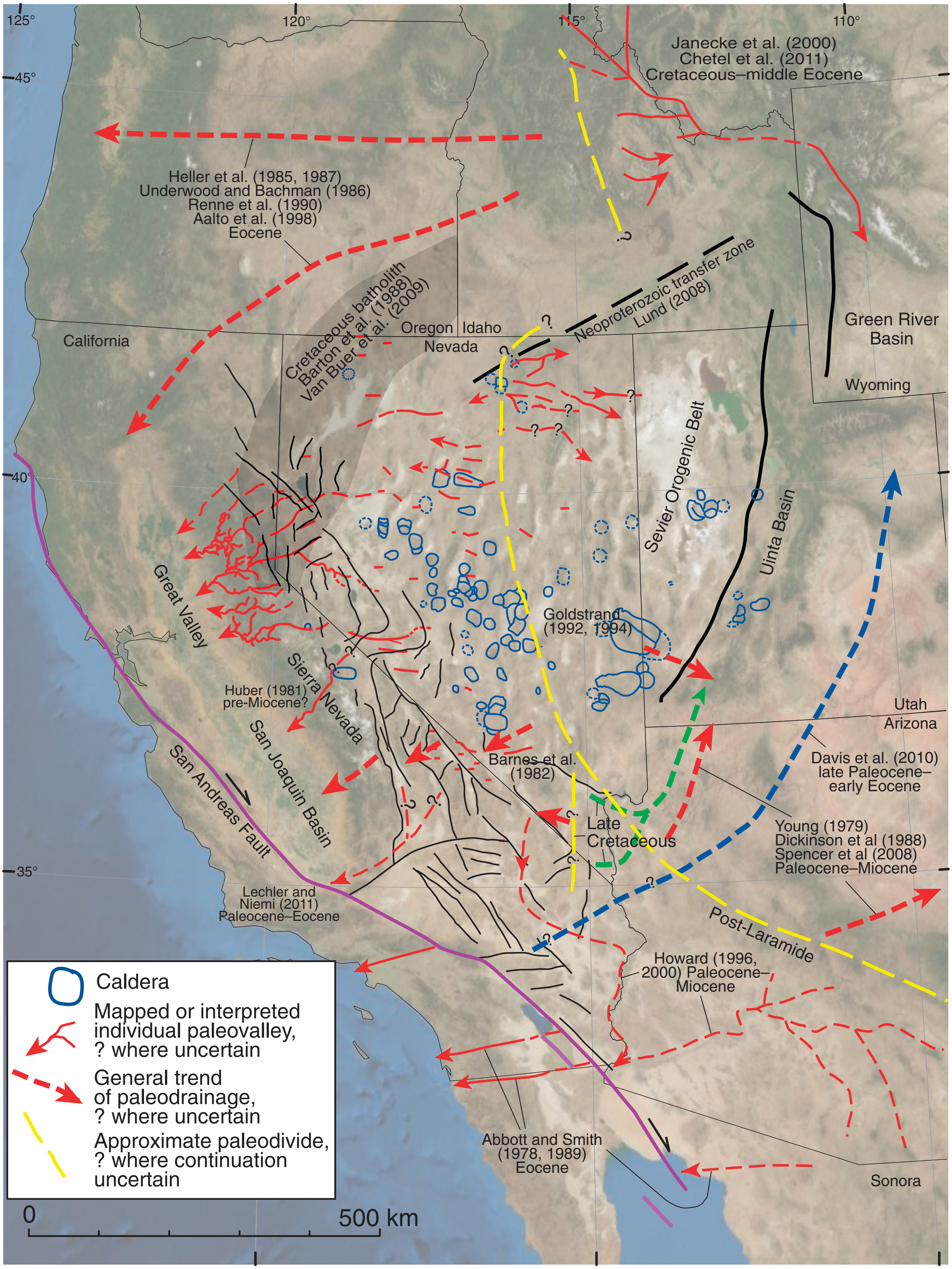

125°
120°
115°
110°
45°
40°
35°
Janecke et al. (2000)
Chetel et al. (2011)
Cretaceous–middle Eocene
Heller et al. (1985, 1987)
Underwood and Bachman (1986)
Renne et al. (1990)
Aalto et al. (1998)
Eocene
Cretaceous batholith
Barton et al. (1988)
Van Buer et al. (2009)
Neoproterozoic transfer zone
Lund (2008)
Green River Basin
Wyoming
California
Oregon
Idaho
Nevada
Sevier Orogenic Belt
Uinta Basin
Great Valley
Goldstrand (1992, 1994)
Sierra Nevada
Huber (1981) pre-Miocene?
San Joaquin Basin
San Andreas Fault
Barnes et al. (1982)
Late Cretaceous
Utah
Arizona
Davis et al. (2010) late Paleocene–early Eocene
Young (1979)
Dickinson et al (1988)
Spencer et al (2008)
Paleocene–Miocene
Lechler and Niemi (2011) Paleocene–Eocene
Post-Laramide
Howard (1996, 2000) Paleocene–Miocene
Abbott and Smith (1978, 1989) Eocene
Sonora
Caldera
Mapped or interpreted individual paleovalley, ? where uncertain
General trend of paleodrainage, ? where uncertain
Approximate paleodivide, ? where continuation uncertain
0
500 km

Figure 11.

indicates rapid cooling and exhumation into the Paleogene, much slower cooling beginning by ca. 45 Ma, and exhumation related to rifting in the Gulf of California in the Late Miocene (Seiler et al., 2011). The cooling history and interpreted exhumation is similar to but displaced slightly younger than those for the Sierra Nevada (Cecil et al., 2006; Seiler et al., 2011). The thermochronology suggests that paleodrainages across the Peninsular Ranges were established at least by ca. 45 Ma, consistent with the Eocene age of deposits in the drainages, and could have been maintained into the Late Miocene, although upstream parts in Arizona and Sonora were probably disrupted by Oligocene–Early Miocene extension (Spencer et al., 1995; Gans, 1997).

These observations suggest that the location of the early to middle Cenozoic paleodivide was controlled to the north largely by uplift of the Sevier orogenic belt, whereas to the south it was largely controlled by the locus of Laramide deformation, which partly overprinted the Sevier belt and altered older drainage. Cenozoic magmatism everywhere postdates formation of the paleovalleys, so the processes that generated magmatism, including rollback of the shallow Farallon slab, did not generate the Nevadaplano. In particular, the caldera-batholith belt of the ignimbrite flareup (Best et al., 1989) long postdates the paleodrainages and does not correlate spatially with the paleodivide, so was not a significant influence on regional paleotopography. Establishment of paleodrainages along the entire length of the paleodivide by the Paleocene seems to contradict the interpretation that uplift migrated southward with magmatism (Mix et al., 2011).

From stable isotope data, Mix et al. (2011) interpreted that uplift to 3–4 km elevation swept southward through the North American Cordillera during the Eocene as a result of removal of the Farallon slab. Although Mix et al. (2011) conceded that a late Mesozoic Nevadaplano highland may have formed as a result of crustal thickening from contraction, they interpreted most uplift to be in the Eocene and that maximum elevations were reached in the Eocene–Oligocene. Ash-flow tuff and paleovalley distributions do not constrain absolute elevations, and so do not confirm or deny this interpretation. However, lack of significant paleovalley incision during magmatism seems more consistent with little surface uplift at that time.

CONCLUSIONS

1. The 28.9 Ma tuff of Campbell Creek erupted from a caldera in north-central Nevada and spread through paleovalleys across northern Nevada and the Sierra Nevada, over a modern area of at least 55,000 km^2. Corrected for later extension, the tuff flowed at least ~200 km to the west, downvalley and across what is now the Basin and Range–Sierra Nevada structural and topographic boundary to the western foothills of the Sierra Nevada, and ~215 km to the northeast, partly upvalley, across an inferred paleodivide, and downvalley to the east to the present East Humboldt Range in northeastern Nevada. With the Nine Hill and Peach Springs Tuffs, the tuff of Campbell Creek is one of the most extensive tuffs of western North America.

2. The distribution of the tuff of Campbell Creek and other middle Cenozoic ash-flow tuffs supports the concept that what is now the Great Basin was an erosional highland, commonly referred to as the Nevadaplano, with a north-south paleodivide through east-central Nevada. Major rivers drained westward to the Pacific Ocean and eastward, probably to the Uinta Basin.

3. The Sierra Nevada was the western flank of this erosional highland in the middle Cenozoic. Paleodrainages definitely crossed the northern and central Sierra Nevada and may have crossed the southern Sierra Nevada.

4. Based on comparison with Quaternary ash-flow tuffs, the great flow distances of middle Cenozoic tuffs do not require, but also do not preclude, that the erosional highland be much higher than ~1.5 km.

5. Major extension that dismembered the highland and generated Basin and Range structure and topography had to be mostly post–23 Ma in western Nevada and post–29 Ma in northeastern Nevada, including in the region of the Ruby Mountains metamorphic core complex.

6. The erosional highland extended at least from Idaho to northern Sonora, Mexico, and probably mostly resulted from Sevier contraction, overprinted by Laramide contraction in and south of southern Nevada.

ACKNOWLEDGMENTS

Myron Best's pointing out to us in 2001 the section of Bates Mountain Tuff in the Reese River Narrows was a key event leading to this paper; examination of that section was probably the greatest, earliest clue of the wide distribution of the tuff of Campbell Creek. We thank Sherman Gromme for patiently pointing out the paleomagnetic match between the "C" unit of Bates Mountain Tuff and the tuff of Campbell Creek. We also thank Jim Wood, Brian Hausback, and Al Deino for discussions about ash-flow tuffs and paleotopography in the Sierra Nevada. The $^{40}Ar/^{39}Ar$ ages were determined at the New Mexico Geochronology Research Laboratory (New Mexico Institute of Mining and Technology) under the patient guidance of Bill McIntosh, Matt Heizler, Lisa Peters, and Rich Esser. We thank Myron Best and Peter DeCelles for thorough, constructive reviews.

REFERENCES CITED

Aalto, K.R., Sharp, W.D., and Renne, P.R., 1998, $^{40}Ar/^{39}Ar$ dating of detrital micas from Oligocene–Pleistocene sandstones of the Olympic Peninsula, Klamath Mountains, and northern California Coast Ranges: Provenance and paleodrainage patterns: Canadian Journal of Earth Sciences, v. 35, p. 735–745, doi: 10.1139/e98-025.

Abbott, P.L., and Smith, T.E., 1978, Trace-element comparison of clasts in Eocene conglomerates, southwestern California and northwestern Mexico: Journal of Geology, v. 86, p. 753–762, doi: 10.1086/649742.

Abbott, P.L., and Smith, T.E., 1989, Sonora, Mexico, source for the Eocene Poway Conglomerate of southern California: Geology, v. 17, p. 329–332, doi: 10.1130/0091-7613(1989)017<0329:SMSFTE>2.3.CO;2.

Allen, V.T., 1929, The Ione Formation of California: Berkeley: University of California Department of Geological Sciences Bulletin, v. 18, p. 347–448.

Bailey, R.A., 1989, Geologic map of Long Valley caldera, Mono-Inyo craters volcanic chain, and vicinity, eastern California: U.S. Geological Survey Miscellaneous Investigations Series I-1933, scale 1:62,500.

Barnes, H., Ekren, E.B., Rogers, C.L., and Hedlund, D.C., 1982, Geologic and tectonic maps of the Mercury quadrangle, Nye and Clark Counties, Nevada: U.S. Geological Survey Miscellaneous Investigation Series Map I-1197, scale 1:24,000.

Barrows, K.J., 1971, Geology of the southern Desatoya Mountains, Churchill and Lander Counties, Nevada [Ph.D. thesis]: Los Angeles, University of California, 349 p.

Barton, M.D., Battles, D.A., Debout, C.E., Capo, R.C., Christensen, J.N., Davis, S.R., Hanson, R.B., Michelson, C.J., and Trim, H.G., 1988, Mesozoic contact metamorphism in the western United States, *in* Ernst, W.G., ed., Metamorphism and crustal evolution of the western United States: Rubey Volume 7: Englewood Cliffs, New Jersey, Prentice Hall, p. 110–178.

Bartow, J.A., and McDougall, K., 1984, Tertiary stratigraphy of the southeastern San Joaquin Valley, California: U.S. Geological Survey Bulletin 1529-J, 41 p.

Bateman, P.C., 1992, Plutonism in the central part of the Sierra Nevada batholith, California: U.S. Geological Survey Professional Paper 1483, 186 p.

Bateman, P.C., and Wahrhaftig, C., 1966, Geology of the Sierra Nevada, *in* Bailey, E.H., ed., Geology of northern California: California Division of Mines and Geology Bulletin 190, p. 107–172.

Beard, L.S., 1996, Paleogeography of the Horse Spring Formation in relation to the Lake Mead fault system, Virgin Mountains, Nevada and Arizona, *in* Beratan, K.K., ed., Reconstructing the history of Basin and Range extension using sedimentology and stratigraphy: Geological Society of America Special Paper 303, p. 27–60, doi: 10.1130/0-8137-2303-5.27.

Beard, L.S., Young, R.A., and Faulds, J.E., 2010, Structure, paleogeography, and extensional foundering of the Kingman uplift, northwest Arizona and southeast Nevada: Geological Society of America Abstracts with Programs, v. 42, no. 5, p. 75.

Bent, J.V., 1988, Paleotectonics and provenance of Tertiary sandstones of the San Joaquin Basin, California, *in* Graham, S.A., and Olsen, H.C., eds., Studies of the geology of the San Joaquin Basin: Pacific Section, Society of Economic Paleontologists and Mineralogists Book 60, p. 109–127.

Berner, R.A., and Kothavala, Z., 2001, GEOCARB III: A revised model of atmospheric CO_2 over Phanerozoic time: American Journal of Science, v. 301, p. 182–204, doi: 10.2475/ajs.301.2.182.

Best, M.G., Christiansen, E.H., Deino, A.L., Grommé, C.S., McKee, E.H., and Noble, D.C., 1989, Excursion 3A: Eocene through Miocene volcanism in the Great Basin of the western United States, *in* Chapin, C.E., and Zidek, J., eds., Field excursions to volcanic terranes in the western United States, Volume II: Cascades and intermountain west: New Mexico Bureau of Mines and Mineral Resources Memoir 47, p. 91–133.

Best, M.G., Christiansen, E.H., Deino, A.L., Gromme, C.S., and Tingey, D.G., 1995, Correlation and emplacement of a large, zoned, discontinuously exposed ash flow sheet: The ^{40}Ar chronology, paleomagnetism, and petrology of the Pahranagat Formation, Nevada: Journal of Geophysical Research, v. 100, p. 24,593–24,609, doi: 10.1029/95JB01690.

Best, M.G., Barr, D.L., Christiansen, E.H., Gromme, S., Deino, A.L., and Tingey, D.G., 2009, The Great Basin Altiplano during the middle Cenozoic ignimbrite flareup: Insights from volcanic rocks: International Geology Review, v. 51, p. 589–633, doi: 10.1080/00206810902867690.

Bohannon, R.G., 1984, Nonmarine sedimentary rocks of Tertiary age in the Lake Mead region, southeastern Nevada and northwestern Arizona: U.S. Geological Survey Professional Paper 1259, 72 p.

Brooks, E.R., Wood, M.M., Boehme, D.R., Potter, K.L., and Marcus, B.I., 2003, Geologic map of the Haskell Peak area, Sierra County, California: California Geological Survey Map Sheet 55, scale 1:24,000.

Brooks, E.R., Henry, C.D., and Faulds, J.E., 2008, Age and character of silicic ash-flow tuffs at Haskell Peak, Sierra County, California: Part of a major Eocene(?)–Oligocene paleovalley spanning the Sierra Nevada–Basin and Range boundary: California Geological Survey Map Sheet 55A, scale 1:24,000, 39 p.

Brooks, W.E., Thorman, W.E., and Snee, L.W., 1995, The ^{40}Ar/^{39}Ar ages and tectonic setting of the middle Eocene northeast Nevada volcanic field: Journal of Geophysical Research, v. 100, p. 10,403–10,416, doi: 10.1029/94JB03389.

Buesch, D.C., 1992, Incorporation and redistribution of locally derived lithic fragments within a pyroclastic flow: Geological Society of America, v. 104, p. 1193–1207, doi: 10.1130/0016-7606(1992)104<1193:IAROLD>2.3.CO;2.

Busby, C.J., DeOreo, S.B., Skilling, I., Gans, P.B., and Hagan, J.C., 2008, Carson Pass–Kirkwood paleocanyon system: Paleogeography of the ancestral Cascades arc and implications for landscape evolution of the Sierra Nevada (California): Geological Society of America Bulletin, v. 120, p. 274–299, doi: 10.1130/B25849.1.

California Geological Survey, 2009, Geological hazard notice: Smectite clay deposits in Sierra Nevada foothills: California Geological Survey GeoHazard Notice 2009–001, 4 p.

Cas, R.A.F., and Wright, J.V., 1987, Volcanic successions; modern and ancient: London, Allen and Unwin, 528 p.

Cassel, E.J., and Graham, S.A., 2011, Paleovalley morphology and fluvial system evolution of Eocene–Oligocene sediments ("auriferous gravels"), northern Sierra Nevada, California: Implications for climate, tectonics, and topography: Geological Society of America Bulletin, v. 123, p. 1699–1719, doi: 10.1130/B30356.1.

Cassel, E.J., Calvert, A., and Graham, S.A., 2009a, Age, geochemical composition, and distribution of Oligocene ignimbrites in the northern Sierra Nevada, California: Implications for landscape morphology, elevation, and drainage divide geography of the Nevadaplano: International Geology Review, v. 51, p. 723–742, doi: 10.1080/00206810902880370.

Cassel, E.J., Graham, S.A., and Chamberlain, C.P., 2009b, Cenozoic tectonic and topographic evolution of the northern Sierra Nevada, California, through stable isotope paleoaltimetry in volcanic glass: Geology, v. 37, p. 547–550, doi: 10.1130/G25572A.1.

Cassel, E.J., Henry, C.D., Graham, S.A., and Chamberlain, P.C., 2010, Determining Oligocene topography and tectonism across the northern Sierra Nevada and western Basin and Range using stable isotope paleoaltimetry in volcanic glass: Geological Society of America Abstracts with Programs, v. 42, no. 5, p. 184.

Cassel, E.J., Graham, S.A., Chamberlain, C.P., and Henry, C.D., 2012a, Early Cenozoic topography, morphology, and tectonics of the northern Sierra Nevada and western Basin and Range: Geosphere, v. 8, doi:10.1130/GES00671.1 (in press).

Cassel, E.J., Grove, M., and Graham, S.A., 2012b, Eocene drainage evolution and erosion of the Sierra Nevada batholith across northern California and Nevada: American Journal of Science (in press).

Cecil, M.R., Ducea, M.N., Reiners, P.W., and Chase, C.G., 2006, Cenozoic exhumation of the northern Sierra Nevada, California, from (U-Th)/He thermochronology: Geological Society of America Bulletin, v. 118, p. 1481–1488, doi: 10.1130/B25876.1.

Cecil, M.R., Ducea, M.N., Reiners, P., Gehrels, G., Mulch, A., Allen, C., and Campbell, I., 2010, Provenance of Eocene river sediments from the central northern Sierra Nevada and implications for paleotopography: Tectonics, v. 29, TC6010, doi: 10.1029/2010TC002717.

Cemen, I., Wright, L.A., and Prave, A.R., 1999, Stratigraphy and tectonic implications of the latest Oligocene and early Miocene sedimentary succession, southernmost Funeral Mountains, Death Valley region, California, *in* Wright, L.A., and Troxel, B.W., eds., Cenozoic basins of the Death Valley region: Geological Society of America Special Paper 333, p. 65–86, doi: 10.1130/0-8137-2333-7.65.

Chetel, L.M., Janecke, S.U., Carroll, A.R., Beard, B.L., Johnson, C.M., and Singer, B.S., 2011, Paleogeographic reconstruction of the Eocene Idaho River, North American Cordillera: Geological Society of America Bulletin, v. 123, p. 71–88, doi: 10.1130/B30213.1.

Clark, M.K., Maheo, G., Saleeby, J., and Farley, K.A., 2005, The non-equilibrium landscape of the southern Sierra Nevada, California: GSA Today, v. 15, p. 4–10, doi: 10.1130/1052-5173(2005)015[4:TNLOTS]2.0.CO;2.

Colgan, J.P., 2011, Two-stage model for exhumation of the Ruby Mountains–East Humboldt metamorphic core complex: Geological Society of America Abstracts with Programs, v. 43, no. 4, p. 4.

Colgan, J.P., and Henry, C.D., 2009, Rapid middle Miocene collapse of the Sevier orogenic plateau in north-central Nevada: International Geology Review, v. 51, p. 920–961, doi: 10.1080/00206810903056731.

Colgan, J.P., Howard, K.A., Fleck, R.J., and Wooden, J.L., 2010, Rapid middle Miocene extension and unroofing of the southern Ruby Mountains, Nevada: Tectonics, v. 29, TC6022, doi: 10.1029/2009TC002655.

Cousens, B., Prytulak, J., Henry, C.D., Alcazar, A., and Brownrigg, T., 2008, The geology and geochemistry of the Miocene–Pliocene Ancestral Cascades arc, northern Sierra Nevada, California and Nevada: The roles of the upper mantle, subducting slab, and the Sierra Nevada lithosphere: Geosphere, v. 4, p. 829–853, doi: 10.1130/GES00166.1.

Cousens, B.L., Henry, C.D., Harvey, B.J., Brownrigg, T., Prytulak, J., and Allan, J.F., 2011, Secular variations in magmatism during a continental arc to post-arc transition: Plio-Pleistocene volcanism in the Lake Tahoe/Truckee area, northern Sierra Nevada, California: Lithos, v. 123, p. 225–242, doi: 10.1016/j.lithos.2010.09.009.

Creely, S., and Force, E.R., 2007, Type region of the Ione Formation (Eocene), central California: Stratigraphy, paleogeography, and relation to Auriferous Gravels: U.S. Geological Survey Open-File Report 2006–1378, 65 p.

Crowley, B.E., Koch, P.L., and Davis, E.B., 2008, Stable isotope constraints on the elevation history of the Sierra Nevada Mountains, California: Geological Society of America Bulletin, v. 120, p. 588–598, doi: 10.1130/B26254.1.

Davis, S.J., Dickinson, W.R., Gehrels, G.E., Spencer, J.E., Lawton, T.F., and Carroll, A.R., 2010, The Paleogene California River: Evidence of Mojave-Uinta paleodrainage from U-Pb ages of detrital zircons: Geology, v. 38, p. 931–934, doi: 10.1130/G31250.1.

DeCelles, P.G., 1988, Middle Cenozoic depositional, tectonic, and sea level history of southern San Joaquin Basin, California: American Association of Petroleum Geologists Bulletin, v. 72, p. 1297–1322.

DeCelles, P.G., 2004, Late Jurassic to Eocene evolution of the Cordilleran thrust belt and foreland basin system, western USA: American Journal of Science, v. 304, p. 105–168, doi: 10.2475/ajs.304.2.105.

Deino, A.L., 1985, Stratigraphy, chemistry, K-Ar dating, and paleomagnetism of the Nine Hill Tuff, California-Nevada [Ph.D. thesis]: Berkeley, University of California, 457 p.

Deino, A.L., 1989, Single crystal ^{40}Ar/^{39}Ar dating as an aid in correlation of ash flows: Examples from the Chimney Springs/New Pass Tuffs and the Nine Hill/Bates Mountain Tuffs of California and Nevada: New Mexico Bureau of Mines and Mineral Resources Continental Magmatism Abstracts Bulletin, v. 131, p. 70.

Dickinson, W.R., 2006, Geotectonic evolution of the Great Basin: Geosphere, v. 2, p. 353–368, doi: 10.1130/GES00054.1.

Dickinson, W.R., Klute, M.A., Hayes, M.J., Janecke, S.U., Lundin, E.R., McKittrick, M.A., and Olivares, M.D., 1988, Paleogeographic and paleotectonic setting of Laramide sedimentary basins in the central Rocky Mountain region: Geological Society of America Bulletin, v. 100, p. 1023–1039, doi: 10.1130/0016-7606(1988)100<1023:PAPSOL>2.3.CO;2.

Dilek, Y., and Moores, E.M., 1999, A Tibetan model for the early Tertiary western United States: Geological Society of London Journal, v. 156, p. 929–941, doi: 10.1144/gsjgs.156.5.0929.

Druschke, P., Hanson, A.D., and Wells, M., 2009, Structural, stratigraphic, and geochronologic evidence for extension predating Palaeogene volcanism in the Sevier hinterland, east-central Nevada: International Geology Review, v. 51, p. 743–775, doi: 10.1080/00206810902917941.

Ducea, M.N., 2001, The California arc: Thick granitic batholiths, eclogitic residues, lithospheric-scale thrusting, and magmatic flare-ups: GSA Today, v. 11, p. 4–10, doi: 10.1130/1052-5173(2001)011<0004:TCATGB>2.0.CO;2.

Ducea, M.N., and Saleeby, J.B., 1998, A case for delamination of the deep batholithic crust beneath the Sierra Nevada, California: International Geology Review, v. 40, p. 78–93, doi: 10.1080/00206819809465199.

Dumitru, T.A., 1990, Subnormal Cenozoic geothermal gradients in the extinct Sierra Nevada magmatic arc: Consequences of Laramide and post-Laramide shallow-angle subduction: Journal of Geophysical Research, v. 95, p. 4925–4941, doi: 10.1029/JB095iB04p04925.

Ernst, W.G., 2010, Young convergent-margin orogens, climate, and crustal thickness—A Late Cretaceous–Paleogene Nevadaplano in the American Southwest?: Lithosphere, v. 2, p. 67–75, doi: 10.1130/L84.1.

Farmer, G.L., Glazner, A.F., and Manley, C.R., 2002, Did lithospheric delamination trigger late Cenozoic potassic volcanism in the southern Sierra Nevada, California: Geological Society of America Bulletin, v. 114, p. 754–782, doi: 10.1130/0016-7606(2002)114<0754:DLDTLC>2.0.CO;2.

Faulds, J.E., Feuerbach, D.L., Miller, C.F., and Smith, E.I., 2001, Cenozoic evolution of the northern Colorado River extensional corridor, southern Nevada and northwest Arizona: Pacific Section, American Association of Petroleum Geologists Publication GB 78, p. 239–272.

Faulds, J.E., Henry, C.D., and Hinz, N.H., 2005, Kinematics of the northern Walker Lane: An incipient transform fault along the Pacific–North American plate boundary: Geology, v. 33, p. 505–508, doi: 10.1130/G21274.1.

Ferguson, C.A., 2008, Silver Creek caldera, probable source of the Miocene Peach Spring Tuff, Oatman Mining District, Arizona: Geological Society of America Abstracts with Programs, v. 40, no. 1, p. 33.

Figueroa, A.M., and Knott, J.R., 2010, Tectonic geomorphology of the southern Sierra Nevada Mountains (California): Evidence for uplift and basin formation: Geomorphology, v. 123, p. 34–45, doi: 10.1016/j.geomorph.2010.06.009.

Flowers, R.M., Wernicke, B.P., and Farley, K.A., 2008, Unroofing, incision, and uplift history of the southwestern Colorado Plateau from apatite (U-Th)/He thermochronometry: Geological Society of America Bulletin, v. 120, p. 571–587, doi: 10.1130/B26231.1.

Gans, P.B., 1997, Large-magnitude Oligo-Miocene extension in southern Sonora: Implications for the tectonic evolution of northwest Mexico: Tectonics, v. 16, p. 388–408, doi: 10.1029/97TC00496.

Garside, L.J., Henry, C.D., Faulds, J.E., and Hinz, N.H., 2005, The upper reaches of the Sierra Nevada auriferous gold channels, *in* Rhoden, H.N., et al., eds., Window to the world: Reno, Geological Society of Nevada Symposium Proceedings, p. 209–235.

Glazner, A.F., Nielson, J.E., Howard, K.A., and Miller, D.M., 1986, Correlation of the Peach Springs Tuff, a large-volume Miocene ignimbrite sheet in California and Arizona: Geology, v. 14, p. 840–843, doi: 10.1130/0091-7613(1986)14<840:COTPST>2.0.CO;2.

Goldstrand, P.M., 1992, Evolution of Late Cretaceous and early Tertiary basins of southwest Utah based on clastic petrology: Journal of Sedimentary Research, v. 62, p. 495–507, doi: 10.1306/D4267933-2B26-11D7-8648000102C1865D.

Goldstrand, P.M., 1994, Tectonic development of Upper Cretaceous to Eocene strata of southwestern Utah: Geological Society of America Bulletin, v. 106, p. 145–154, doi: 10.1130/0016-7606(1994)106<0145:TDOUCT>2.3.CO;2.

Gonsior, Z.J., and Dilles, J.H., 2008, timing and evolution of Cenozoic extensional normal faulting and magmatism in the southern Tobin Range, Nevada: Geosphere, v. 4, p. 687–712, doi: 10.1130/GES00137.1.

Graham, S.A., and Olsen, H.C., eds., 1988, Studies of the geology of the San Joaquin Basin: Pacific Section, Society of Economic Paleontologists and Mineralogists Book 60, 351 p.

Gromme, C.S., McKee, E.H., and Blake, M.C., Jr., 1972, Paleomagnetic correlations and potassium-argon dating of middle Tertiary ash-flow sheets in the eastern Great Basin, Nevada and Utah: Geological Society of America Bulletin, v. 83, p. 1619–1638, doi: 10.1130/0016-7606(1972)83[1619:PCAPDO]2.0.CO;2.

Hanson, A.D., 2008, Detrital zircon constraints on the Jean conglomerate and Sevier unroofing near Las Vegas: Geological Society of America Abstracts with Programs, v. 40, no. 1, p. 56.

Harding, J.P., Gehrels, G.E., Harwood, D.S., and Girty, G.H., 2000, Detrital zircon geochronology of the Shoo Fly Complex, northern Sierra terrane, northeastern California, *in* Soreghan, M.J., and Gehrels, G.E., eds., Paleozoic and Triassic paleogeography and tectonics of western Nevada and northern California: Geological Society of America Special Paper 347, p. 43–55, doi: 10.1130/0-8137-2347-7.43.

Hay, D.C., and Dempster, T.J., 2009, Zircon alteration, formation and preservation in sandstones: Sedimentology, v. 56, p. 2175–2191, doi: 10.1111/j.1365-3091.2009.01075.x.

Haynes, S.R., 2003, Development of the Eocene Elko basin, northeastern Nevada: Implications for paleogeography and regional tectonism [M.S. thesis]: Vancouver, University of British Columbia, 159 p.

Heller, P.L., Peterman, Z.E., O'Neil, J.R., and Shafiqullah, M., 1985, Isotopic provenance of sandstone from the Eocene Tyee Formation, Oregon Coast Range: Geological Society of America Bulletin, v. 96, p. 770–780, doi: 10.1130/0016-7606(1985)96<770:IPOSFT>2.0.CO;2.

Heller, P.L., Tabor, R.W., and Suczek, C.A., 1987, Paleogeographic evolution of the United States Pacific Northwest during Paleogene time: Canadian Journal of Earth Sciences, v. 24, p. 1652–1667, doi: 10.1139/e87-159.

Henry, C.D., 2008, Ash-flow tuffs and paleovalleys in northeastern Nevada: Implications for Eocene paleogeography and extension in the Sevier hinterland, northern Great Basin: Geosphere, v. 4, p. 1–35, doi: 10.1130/GES00122.1.

Henry, C.D., and Faulds, J.E., 2010, Ash-flow tuffs in the Nine Hill, Nevada, paleovalley and implications for tectonism and volcanism of the western Great Basin, USA: Geosphere, v. 6, p. 339–369, doi: 10.1130/GES00548.1.

Henry, C.D., McGrew, A.J., Colgan, J.P., Snoke, A.W., and Brueseke, M.E., 2011, Timing, distribution, amount, and style of Cenozoic extension in the northern Great Basin, *in* Lee, J., and Evans, J.P., eds., Geologic field trips to the Basin and Range, Rocky Mountains, Snake River Plain, and terranes of the U.S. Cordillera: Geological Society of America Field Guide 21, p. 27–66.

Hildreth, W., and Wilson, C.J.N., 2007, Compositional zoning of the Bishop Tuff: Journal of Petrology, v. 48, p. 951–999, doi: 10.1093/petrology/egm007.

Hinz, N.H., Faulds, J.E., and Henry, C.D., 2009, Tertiary volcanic stratigraphy and paleotopography of the Diamond and Fort Sage Mountains, northeastern California and western Nevada—Implications for development of the northern Walker Lane, *in* Oldow, J.S., and Cashman, P.H., eds., Late Cenozoic structure and evolution of the Great Basin–Sierra Nevada transition: Geological Society of America Special Paper 447, p. 101–132, doi: 10.1130/2009.2447(07).

Horton, T.W., and Chamberlain, C.P., 2006, Stable isotopic evidence for Neogene surface downdrop in the central Basin and Range Province: Geological Society of America Bulletin, v. 118, p. 475–490, doi: 10.1130/B25808.

Horton, T.W., Sjostrom, D.J., Abruzzese, M.J., Poage, M.A., Waldbauer, J.R., Hren, M., Wooden, J., and Chamberlain, C.P., 2004, Spatial and temporal variation of Cenozoic surface elevation in the Great Basin and Sierra Nevada: American Journal of Science, v. 304, p. 862–888, doi: 10.2475/ajs.304.10.862.

Hoskin, P.O., and Schaltegger, U., 2003, The composition of zircon and igneous and metamorphic petrogenesis, *in* Hanchar, J.M., and Hoskin, P.W.O., eds., Zircon: Mineralogical Society of America Reviews in Mineralogy and Geochemistry 53, p. 27–62.

House, M.A., Wernicke, B.P., Farley, K.A., and Dumitru, T.A., 1997, Cenozoic thermal evolution of the central Sierra Nevada, California, from (U-Th)/He thermochronometry: Earth and Planetary Science Letters, v. 151, p. 167–179, doi: 10.1016/S0012-821X(97)81846-8.

Howard, J.L., 1996, Paleocene to Holocene paleodeltas of ancestral Colorado River offset by the San Andreas fault system, southern California: Geology, v. 24, p. 783–786, doi: 10.1130/0091-7613(1996)024<0783:PTHPOA>2.3.CO;2.

Howard, J.L., 2000, Provenance of quartzite clasts in the Eocene–Oligocene Sespe Formation: Paleogeographic implications for southern California and the ancestral Colorado River: Geological Society of America Bulletin, v. 112, p. 1635–1649, doi: 10.1130/0016-7606(2000)112<1635:POQCIT>2.0.CO;2.

Howard, K.A., 2003, Crustal structure in the Elko-Carlin region, Nevada, during Eocene gold mineralization: Ruby–East Humboldt metamorphic core complex as a guide to the deep crust: Economic Geology and the Bulletin of the Society of Economic Geologists, v. 98, p. 249–268, doi: 10.2113/98.2.249.

Hren, M.T., Pagani, M., Erwin, D.M., and Brandon, M., 2010, Biomarker reconstruction of the early Eocene paleotopography and paleoclimate of the northern Sierra Nevada: Geology, v. 38, p. 7–10, doi: 10.1130/G30215.1.

Huber, N.K., 1981, Amount and timing of late Cenozoic uplift and tilt of the central Sierra Nevada, California—Evidence from the upper San Joaquin River basin: U.S. Geological Survey Professional Paper 1197, 28 p.

Hudson, M.R., and Geissman, J.W., 1991, Paleomagnetic evidence for the age and extent of middle Tertiary counterclockwise rotation, Dixie Valley region, west-central Nevada: Journal of Geophysical Research, v. 96, p. 3979–4006, doi: 10.1029/90JB02424.

Humphreys, E.D., Hessler, E., Dueker, K., Farmer, G.L., Erslev, E., and Atwater, T., 2003, How Laramide-age hydration of North American lithosphere by the Farallon slab controlled subsequent activity in the western United States: International Geology Review, v. 45, p. 575–595, doi: 10.2747/0020-6814.45.7.575.

Janecke, S.U., VanDenburg, C.J., Blankenau, J.J., and M'Gonigle, J.W., 2000, Long-distance longitudinal transport of gravel across the Cordilleran thrust belt of Montana and Idaho: Geology, v. 28, p. 439–442, doi: 10.1130/0091-7613(2000)28<439:LLTOGA>2.0.CO;2.

Jenkins, O.P., 1932, Geologic map of northern Sierra Nevada showing Tertiary river channels and mother lode belt, *in* Bradley, W.W., ed., 28th Report of the State Mineralogist: California Division of Mines and Geology, p. 279–298.

John, D.A., 1992, Stratigraphy, regional distribution, and reconnaissance geochemistry of Oligocene and Miocene volcanic rocks in the Paradise Range and northern Pactolus Hills, Nye County, Nevada: U.S. Geological Survey Bulletin 1974, 67 p.

John, D.A., 1995, Tilted middle Tertiary ash-flow calderas and subjacent granitic plutons, southern Stillwater Range, Nevada: Cross sections of an Oligocene igneous center: Geological Society of America Bulletin, v. 107, p. 180–200, doi: 10.1130/0016-7606(1995)107<0180:TMTAFC>2.3.CO;2.

John, D.A., Henry, C.D., and Colgan, J.P., 2008a, Magmatic and tectonic evolution of the Caetano caldera, north-central Nevada: A tilted mid-Tertiary eruptive center and source of the Caetano Tuff: Geosphere, v. 4, p. 75–106, doi: 10.1130/GES00116.1.

John, D.A., Henry, C.D., and Colgan, J.P., 2008b, The Caetano caldera, Nevada: 5 km thickness of intra-caldera rhyolite ignimbrite and co-magmatic batholith: Eos (Transactions, American Geophysical Union), v. 89, no. 52, fall meeting supplement, abs. V21C–2118.

Jones, C.H., Farmer, G.L., and Unruh, J., 2004, Tectonics of Pliocene removal of lithosphere of the Sierra Nevada, California: Geological Society of America Bulletin, v. 116, p. 1408–1422, doi: 10.1130/B25397.1.

Kaneko, K., Kamata, H., Koyaguchi, T., Yoshikawa, M., and Furukawa, K., 2007, Repeated large-scale eruptions from a single compositionally stratified magma chamber: An example from Aso volcano, southwest Japan: Journal of Volcanology and Geothermal Research, v. 167, p. 160–180, doi: 10.1016/j.jvolgeores.2007.05.002.

Kelly, D.C., Zachos, J.C., Bralower, T.J., and Schellenberg, S.A., 2005, Enhanced terrestrial weathering/runoff and surface ocean carbonate production during the recovery stages of the Paleocene-Eocene thermal maximum: Paleoceanography, v. 20, p. 1–11, doi: 10.1029/2005PA001163.

Kohl, M.S., 1978, Tertiary volcanic rocks of the Jean-Sloan area, Clark County, Nevada, and their possible relationship to carnotite occurrences in caliche [M.S. thesis]: Los Angeles, University of California, 116 p.

Kuiper, K.F., Deino, A., Hilgen, F.J., Krijgsman, W., Renne, P.R., and Wijbrans, J.R., 2008, Synchronizing rock clocks of Earth history: Science, v. 320, p. 500–504, doi: 10.1126/science.1154339.

Lamb, M.A., Beard, L.S., Hickson, T., Umhoefer, P.J., Schleicher, J., Kopp, J., and Sitton, M.E., 2011, Oligo-Miocene paleogeography of the Lake Mead region: The Rainbow Gardens Member of the Horse Spring Formation records pre-extensional tectonics of the central Basin and Range: Geological Society of America Abstracts with Programs, v. 43, no. 4, p. 70.

Lease, R.O., McQuarrie, N., Oskin, M., and Leier, A., 2009, Quantifying dextral shear on the Bristol-Granite Mountains fault zone: Successful geologic prediction from kinematic compatibility of the eastern California shear zone: Journal of Geology, v. 117, p. 37–53, doi: 10.1086/593320.

Lechler, A.R., and Niemi, N.A., 2011, Sedimentologic and isotopic constraints on the Paleogene paleogeography and paleotopography of the southern Sierra Nevada, California: Geology, v. 39, p. 379–382, doi: 10.1130/G31535.1.

Lerch, D.W., Klemperer, S.L., Glen, J.M.G., Ponce, D.A., Miller, E.L., and Colgan, J.P., 2007, Crustal structure of the northwestern Basin and Range Province and its transition to unextended volcanic plateaus: Geochemistry Geophysics Geosystems, v. 8, Q02011, doi: 10.1029/2006GC001429, 21 p.

Lindgren, W., 1911, The Tertiary gravels of the Sierra Nevada of California: U.S. Geological Survey Professional Paper 73, 226 p.

Lipman, P.W., 1967, Mineral and chemical variations within an ash-flow sheet from Aso caldera, southwestern Japan: Contributions to Mineralogy and Petrology, v. 16, p. 300–327, doi: 10.1007/BF00371528.

Lund, K., 2008, Geometry of Neoproterozoic and Paleozoic rift margin of western Laurentia: Implications for mineral deposit settings: Geosphere, v. 4, p. 429–444, doi: 10.1130/GES00121.1.

MacGinitie, H.D., 1941, A middle Eocene flora from the central Sierra Nevada: Carnegie Institute of Washington Publication 534, 178 p.

Mason, B.G., Pyle, D.M., and Oppenheimer, C., 2004, The size and frequency of the largest explosive eruptions on Earth: Bulletin of Volcanology, v. 66, p. 735–748, doi: 10.1007/s00445-004-0355-9.

Matumoto, T., 1943, The four gigantic caldera volcanoes of Kyusyu: Japanese Journal of Geology and Geography, v. 19, 57 p.

Maughan, L.L., Christiansen, E.H., Best, M.G., Gromme, C.S., Deino, A.L., and Tingey, D.G., 2002, The Oligocene Lund Tuff, Great Basin, USA: A very large volume monotonous intermediate: Journal of Volcanology and Geothermal Research, v. 113, p. 129–157, doi: 10.1016/S0377-0273(01)00256-6.

McConnell, V.S., Shearer, C.K., Eichelberger, J.C., Keskinen, M.J., Layer, P.W., and Papike, J.J., 1995, Rhyolite intrusions in the intracaldera Bishop Tuff, Long Valley caldera, California: Journal of Volcanology and Geothermal Research, v. 67, p. 41–60, doi: 10.1016/0377-0273(94)00099-3.

McGrew, A.J., and Snee, L.W., 1994, ^{40}Ar/^{39}Ar thermochronologic constraints on the tectonothermal evolution of the northern East Humboldt Range metamorphic core complex, Nevada: Tectonophysics, v. 238, p. 425–450, doi: 10.1016/0040-1951(94)90067-1.

McGrew, A.J., Peters, M.T., and Wright, J.E., 2000, Thermobarometric constraints on the tectonothermal evolution of the East Humboldt Range metamorphic core complex, Nevada: Geological Society of America Bulletin, v. 112, p. 45–60, doi: 10.1130/0016-7606(2000)112<45:TCOTTE>2.0.CO;2.

McIntosh, W.C., Heizler, M., Peters, L., and Esser, R., 2003, ^{40}Ar/^{39}Ar geochronology at the New Mexico Bureau of Geology and Mineral Resources: New Mexico Bureau of Geology and Mineral Resources Open File Report OF-AR-1, 10 p.

McKee, E.H., 1968, Geologic map of the Spencer Hot Springs Quadrangle, Lander and Eureka Counties, Nevada: U.S. Geological Survey Geologic Quadrangle Map GQ-770, scale 1:62,500.

McKee, E.H., and Conrad, J.E., 1987, Geologic map of the Desatoya Mountains Wilderness Study Area, Churchill and Lander Counties, Nevada: U.S. Geological Survey Miscellaneous Field Studies Map MF-1944, scale 1:62,500.

McKee, E.H., and Stewart, J.H., 1971, Stratigraphy and potassium-argon ages of some Tertiary tuffs from Lander and Churchill Counties, central Nevada: U.S. Geological Survey Bulletin 1311-B, 28 p.

Miller, C.F., and Wark, D.A., 2008, Supervolcanoes and their explosive supereruptions: Elements, v. 4, p. 11–16, doi: 10.2113/GSELEMENTS.4.1.11.

Mix, H.T., Mulch, A., Kent-Corson, M.L., and Chamberlain, C.P., 2011, Cenozoic migration of topography in the North American Cordillera: Geology, v. 39, p. 87–90, doi: 10.1130/G31450.1.

Molnar, P., 2010, Deuterium and oxygen isotopes, paleoelevations of the Sierra Nevada, and Cenozoic climate: Geological Society of America Bulletin, v. 122, p. 1106–1115, doi: 10.1130/B30001.1.

Mulch, A., Graham, S.A., and Chamberlain, C.P., 2006, Hydrogen isotopes in Eocene river gravels and paleoelevation of the Sierra Nevada: Science, v. 313, p. 87–89, doi: 10.1126/science.1125986.

Mulch, A., Sarna-Wojcicki, A.M., Perkins, M.E., and Chamberlain, C.P., 2008, A Miocene to Pleistocene climate and elevation record of the Sierra Nevada (California): National Academy of Science Proceedings, v. 105, p. 6819–6824, doi: 10.1073 pnas.0708811105. 105.

Niemi, N.A., 2002, Extensional tectonics in the Basin and Range Province and the geology of the Grapevine Mountains, Death Valley region, California and Nevada [Ph.D. thesis]: Pasadena, California Institute of Technology, 337 p.

Nilsen, T.H., and Clarke, S.H., 1975, Sedimentation and tectonics in the early Tertiary continental borderland of central California: U.S. Geological Survey Professional Paper 925, 64 p.

Pelletier, J.D., 2007, Numerical modeling of the Cenozoic geomorphic evolution of the southern Sierra Nevada, California: Earth and Planetary Science Letters, v. 259, p. 85–96, doi: 10.1016/j.epsl.2007.04.030.

Petronis, M.S., Geissman, J.W., and McIntosh, W.C., 2004, Transitional field clusters from uppermost Oligocene volcanic rocks in the central Walker Lane, western Nevada: Physics of the Earth and Planetary Interiors, v. 141, p. 207–238, doi: 10.1016/j.pepi.2003.12.004.

Proffett, J.M., and Proffett, B., 1976, Stratigraphy of the Tertiary ash-flow tuffs in the Yerington District, Nevada: Nevada Bureau of Mines and Geology Report 27, 28 p.

Renne, P.R., Becker, T.A., and Swapp, S.M., 1990, ^{40}Ar/^{39}Ar laser-probe dating of detrital micas from the Montgomery Creek Formation: Clues to provenance, tectonics, and weathering processes: Geology, v. 18, p. 563–566, doi: 10.1130/0091-7613(1990)018<0563:AALPDO>2.3.CO;2.

Renne, P.R., Swisher, C.C., and Deino, A.L., Karner, D.B., Owens, T.L., and DePaolo, D.J., 1998, Intercalibration of standards, absolute ages and uncertainties in ^{40}Ar/^{39}Ar dating: Chemical Geology, v. 145, p. 117–152, doi: 10.1016/S0009-2541(97)00159-9.

Saleeby, J.B., 2003, Segmentation of the Laramide slab—Evidence from the southern Sierra Nevada region: Geological Society of America Bulletin, v. 115, p. 655–668, doi: 10.1130/0016-7606(2003)115<0655:SOTLSF>2.0.CO;2.

Saleeby, J.B., Ducea, M.N., and Clemens-Knott, D., 2003, Production and loss of high-density batholithic root, southern Sierra Nevada, California: Tectonics, v. 22, 1064, 24 p., doi: 10.1029/2002TC001374.

Saleeby, J.B., Ducea, M.N., Busby, C.J., Nadin, E.S., and Wetmore, P.H., 2008, Chronology of pluton emplacement and regional deformation in the southern Sierra Nevada batholith, California, *in* Wright, J.E., and Shervais, J.W., eds., Ophiolites, arcs, and batholiths: A tribute to Cliff Hopson: Geological Society of America Special Paper 438, p. 397–427, doi: 10.1130/2008.2438(14).

Saleeby, J.B., Saleeby, Z., Liu, L., and Maheo, G., 2010, Mid-Cretaceous regional exhumation of the Sierra Nevada–Great Valley batholith and a possible tectonic driving mechanism: Geological Society of America Abstracts with Programs, v. 42, no. 4, p. 67.

Samson, S.D., and Alexander, E.C., Jr., 1987, Calibration of the interlaboratory ^{40}Ar/^{39}Ar dating standard, MMhb-1: Chemical Geology, v. 66, p. 27–34.

Sargent, K.A., and McKee, E.H., 1969, The Bates Mountain Tuff in northern Nye County, Nevada: U.S. Geological Survey Bulletin 1294-E, 12 p.

Saylor, B.Z., and Hodges, K.V., 1994, ^{40}Ar/^{39}Ar age constraints on the depositional history of the Oligocene Titus Canyon Formation, Death Valley, California: Geological Society of America Abstracts with Programs, v. 26, no. 2, p. 88.

Seiler, C., Fletcher, J.M., Kohn, B.P., Gleadow, A.J.W., and Raza, A., 2011, Low-temperature thermochronology of northern Baja California, Mexico: Decoupled slip-exhumation gradients and delayed onset of oblique rifting across the Gulf of California: Tectonics, v. 30, 24, TC3004, doi: 10.1029/2009TC002649

Slate, J.L., and 29 others, 2000, Digital geologic map of the Nevada Test Site and vicinity, Nye, Lincoln, and Clark Counties, Nevada, and Inyo County, California: U.S. Geological Survey Open-File Report 00–554, scale 1:100,000.

Slemmons, D.B., 1953, Geology of the Sonora Pass region [Ph.D. thesis]: Berkeley, University of California, 222 p.

Snoke, A.W., Howard, K.A., McGrew, A.J., Burton, B.R., Barnes, C.G., Peters, M.T., and Wright, J.E., 1997, The grand tour of the Ruby–East Humboldt metamorphic core complex, northeastern Nevada: Brigham Young University Geological Studies, v. 42, p. 225–269.

Snow, J.K., and Lux, D.R., 1999, Tectono-sequence stratigraphy of Tertiary rocks in the Cottonwood Mountains and northern Death Valley area, California and Nevada, *in* Wright, L.A., and Troxel, B.W., eds., Cenozoic basins of the Death Valley region: Geological Society of America Special Paper 333, p. 17–64, doi: 10.1130/0-8137-2333-7.17.

Snow, J.K., and Wernicke, B.P., 2000, Cenozoic tectonism in the central Basin and Range: Magnitude, rate, and distribution of upper crustal strain: American Journal of Science, v. 300, p. 659–719, doi: 10.2475/ajs.300.9.659.

Soreghan, M.J., and Gehrels, G., eds., 2000, Paleozoic and Triassic paleogeography and tectonics of western Nevada and northern California: Geological Society of America Special Paper 347, 246 p., doi: 10.1130/0-8137-2347-7.

Sparks, R.S.J., Self, S., Grattan, J.P., Oppenheimer, C., Pyle, D.M., and Rymer, H., 2005, Supereruptions: Global effects and future threats. Report of a Geological Society of London Working Group: Geological Society of London, 24 p., http://www.geolsoc.org.uk/gsl/education/page2965.html.

Spencer, J.E., Richard, S.M., Reynolds, S.J., Miller, R.J., Shafiqullah, M., Gilbert, W.G., and Grubensky, M.J., 1995, Spatial and temporal relationships between mid-Tertiary magmatism and extension in southwestern Arizona: Journal of Geophysical Research, v. 100, p. 10,321–10,351, doi: 10.1029/94JB02817.

Spencer, J.E., Smith, G.R., and Dowling, T.E., 2008, Middle to late Cenozoic geology, hydrography, and fish evolution in the American Southwest, *in* Reheis, M.C., et al., eds., Late Cenozoic drainage history of the southwestern Great Basin and lower Colorado River region: Geologic and biotic perspectives: Geological Society of America Special Paper 439, p. 279–299, doi: 10.1130/2008.2439(12).

Spurlin, M.S., Gehrels, G.E., and Harwood, D.S., 2000, Detrital zircon geochronology of upper Paleozoic and lower Mesozoic strata of the northern Sierra terrane, northeastern California, *in* Soreghan, M.J., and Gehrels, G.E., eds., Paleozoic and Triassic paleogeography and tectonics of western Nevada and northern California: Geological Society of America Special Paper 347, p. 89–98, doi: 10.1130/0-8137-2347-7.89.

Steiger, R.H., and Jäger, E., 1977, Subcommission on geochronology: Convention on the use of decay constants in geo- and cosmochronology: Earth and Planetary Science Letters, v. 36, p. 359–362, doi: 10.1016/0012-821X(77)90060-7.

Stewart, J.H., 1980, Geology of Nevada—A discussion to accompany the geologic map of Nevada: Nevada Bureau of Mines and Geology Special Publication 4, 136 p.

Stewart, J.H., and McKee, E.H., 1968, Geologic map of the Mount Callaghan Quadrangle, Lander County, Nevada: U.S. Geological Survey Geologic Quadrangle Map GQ-730, scale 1:62,500.

Stewart, J.H., and McKee, E.H., 1977, Geology and mineral deposits of Lander County, Nevada: Part 1, Geology: Nevada Bureau of Mines and Geology Bulletin 88, 59 p.

Stock, G.M., Anderson, R.S., and Finkel, R.C., 2004, Pace of landscape evolution in the Sierra Nevada, California, revealed by cosmogenic dating of cave sediments: Geology, v. 32, p. 193–196, doi: 10.1130/G20197.1.

Stock, G.M., Anderson, R.S., and Finkel, R.C., 2005, Rates of erosion and topographic evolution of the Sierra Nevada, California, inferred from cosmogenic ^{26}Al and ^{10}Be concentrations: Earth Surface Processes and Landforms, v. 30, p. 985–1006, doi: 10.1002/esp.1258.

Sun, S., and McDonough, W.F., 1989, Chemical and isotopic systematics of oceanic basalts; implications for mantle composition and processes, *in* Saunders, A.D., and Norry, M.J., eds., Magmatism in the ocean basins: Geological Society of London Special Publication 42, p. 315–345.

Umhoefer, P.J., Hickson, T.A., and Lamb, M.A., 2011, Climatic versus tectonic controls on sedimentary facies in the Oligocene–Miocene Horse Springs Formation, Lake Mead domain, Nevada: Geological Society of America Abstracts with Programs, v. 43, no. 4, p. 70.

Underwood, M.B., and Bachman, S.B., 1986, Sandstone petrofacies of the Yager complex and the Franciscan Coastal belt, Paleogene of northern California: Geological Society of America Bulletin, v. 97, p. 809–817, doi: 10.1130/0016-7606(1986)97<809:SPOTYC>2.0.CO;2.

Unruh, J.R., 1991, The uplift of the Sierra Nevada and implications for late Cenozoic epeirogeny in the western Cordillera: Geological Society of America Bulletin, v. 103, p. 1395–1404, doi: 10.1130/0016-7606(1991)103<1395:TUOTSN >2.3.CO;2.

Valentine, G.A., Buesch, D.C., and Fisher, R.V., 1989, Basal layered deposits of the Peach Springs Tuff, northwestern Arizona, USA: Bulletin of Volcanology, v. 51, p. 395–414, doi: 10.1007/BF01078808.

Van Buer, N.J., Miller, E.L., and Dumitru, T.A., 2009, Early Tertiary paleogeologic map of the northern Sierra Nevada batholith and the northwestern Basin and Range: Geology, v. 37, p. 371–374, doi: 10.1130/G25448A.1.

Wakabayashi, J., and Sawyer, T.L., 2001, Stream incision, tectonics, uplift, and evolution of topography of the Sierra Nevada, California: Journal of Geology, v. 109, p. 539–562, doi: 10.1086/321962.

Walker, J.D., and Geissman, J.W., compilers, 2009, Geologic time scale: Geological Society of America, doi: 10.1130/2009.CTS004R2C.

Walker, G.P.L., and Wilson, C.J.N., 1983, Lateral variations in the Taupo Ignimbrite: Journal of Volcanology and Geothermal Research, v. 18, p. 117–133, doi: 10.1016/0377-0273(83)90005-7.

Wernicke, B.P., 2011, The California River and its role in carving Grand Canyon: Geological Society of America Bulletin, v. 123, p. 1288–1316, doi: 10.1130/B30274.1.

Wernicke, B.P., and 18 others, 1996, Origin of high mountains in the continents: The southern Sierra Nevada: Science, v. 271, p. 190–193, doi: 10.1126/science.271.5246.190.

Wilson, M.J., 1999, The origin and formation of clay minerals in soils: Past, present and future perspectives: Clay Minerals, v. 34, p. 7–25, doi: 10.1180/000985599545957.

Wing, S.L., and Greenwood, D.R., 1993, Fossils and fossil climate: The case for equable continental interiors in the Eocene: Royal Society of London Philosophical Transactions, ser. B, v. 341, p. 243–252, doi: 10.1098/rstb.1993.0109.

Wolfe, J.A., Schorn, H.E., Forest, C.E., and Molnar, P., 1997, Paleobotanical evidence for high altitudes in Nevada during the Miocene: Science, v. 276, p. 1672–1675, doi: 10.1126/science.276.5319.1672.

Wood, J.L., 1994, A re-evaluation of the origin of kaolinite in the Ione depositional system (Eocene), Sierra foothills, California [M.S. thesis]: Los Angeles, California State University, 85 p.

Yeend, W.E., 1974, Gold-bearing gravel of the ancestral Yuba River, Sierra Nevada, California: U.S. Geological Survey Professional Paper 772, 44 p.

Young, R.A., 1979, Laramide deformation, erosion and plutonism along the southwestern margin of the Colorado Plateau: Tectonophysics, v. 61, p. 25–47, doi: 10.1016/0040-1951(79)90290-7.

Young, R.A., and Brennan, W.J., 1974, Peach Springs Tuff: Its bearing on structural evolution of the Colorado Plateau and development of Cenozoic drainage in Mohave County, Arizona: Geological Society of America Bulletin, v. 85, p. 83–90, doi: 10.1130/0016-7606(1974)85<83:PSTIBO>2.0.CO;2.

Zachos, J.C., Pagani, M., Sloan, L., Thomas, E., and Billups, K., 2001, Trends, rhythms, and aberrations in global climate 65 Ma to present: Science, v. 292, p. 686–693, doi: 10.1126/science.1059412.

Zandt, G., Gilbert, H., Owens, T.J., Ducea, M., Saleeby, J., and Jones, C.H., 2004, Active foundering of a continental arc root beneath the southern Sierra Nevada in California: Nature, v. 431, p. 41–46, doi: 10.1038/nature02847.

Manuscript Received 2 June 2011
Revised Manuscript Received 21 November 2011
Manuscript Accepted 25 November 2011